The Dissertation Committee for Emily Ann Helton Certifies that this is the approved version of the following dissertation:

feoA, feoB, and *feoC* encode essential components of the *Vibrio cholerae* ferrous iron transport system

Committee:

Shelley M. Payne, Supervisor

Scott W. Stevens

M. Stephen Trent

Marvin Whiteley

Jon Robertus

feoA, *feoB*, and *feoC* encode essential components of the *Vibrio cholerae* ferrous iron transport system

by

Emily Ann Helton, B.S. Med. Tech

Dissertation

Presented to the Faculty of the Graduate School of

The University of Texas at Austin

in Partial Fulfillment

of the Requirements

for the Degree of

Doctor of Philosophy

The University of Texas at Austin

December 2010

Dedication

This work is dedicated to my parents, for your continuous support. To Ben, for listening, for loving, and motivating. Even when far away, you are always there for me.

Acknowledgements

First and foremost, thank you to Shelley Payne for giving me this opportunity and guiding me through. I am grateful to Elizabeth Wyckoff for sharing the Feo project with me, providing reagents, and lots of support and guidance. I would also like to thank Alex Mey for her generosity with reagents, encouragement, and assistance. Thank you to Dr. Scott Stevens for the generous gifts of the plasmid pTAP403 and the antibody to the TAP tag. Thank you to members of the Payne lab, past and present, for all the support over the years. Thank you to Erin Murphy and Nicola Davies, for having always having time to help a new grad student. Many thanks to Aja Gore and Stephanie Craig for years of friendship full of science and laughter.

feoA, *feoB*, and *feoC* encode essential components of the *Vibrio cholerae* ferrous iron transport system

Publication No._____

Emily Ann Helton, Ph.D.

The University of Texas at Austin, 2010

Supervisor: Shelley M. Payne

Vibrio cholerae, the causative agent of the diarrheal disease cholera, must acquire iron to survive. Although iron is relatively abundant, it forms insoluble ferric complexes in the presence of oxygen. The more soluble ferrous iron is limited to anaerobic or reducing environments. To meet the nutritional needs of the cell, *V. cholerae* encodes many different ferric iron transport systems but only one characterized ferrous iron transporter, Feo. Feo is widely distributed in bacteria and archaea, but the mechanism for transport is not known. In this study, basic characterization of the *V. cholerae feoABC* operon was performed to gain further understanding about a critical iron transport system. Each gene in the operon, *feoA, feoB*, and *feoC,* was found to be required for ferrous iron uptake. FeoB, an inner membrane protein, is considered to be the ferrous permease but functions for FeoA and FeoC are not known. These studies show that neither FeoA nor FeoC is required for expression of *feoB*, suggesting that these proteins are required for Feo function. Analysis of the composition of the Feo transporter using a bacterial adenylate cyclase two-hybrid system indicated interactions between Feo

proteins, specifically, between FeoC and the cytoplasmic portion of FeoB. This result indicates that *feoC* encodes a protein that interacts with FeoB and is necessary for ferrous iron transport.

Table of Contents

List of Tables

List of Figures

I. INTRODUCTION

1. Bacterial iron acquisition

Iron exists in two interconvertible redox states, the oxidized ferric or the reduced ferrous state. The ability to convert between these two states makes iron a vital redox component of enzymes involved in important biological processes, including DNA synthesis (6), nitrogen fixation (15) and photosynthesis (37). Due to its role in these processes, iron is essential for almost all organisms. While iron is one of the most abundant elements (81), transport of iron is a complex issue for cells for two reasons. First, iron forms very insoluble ferric complexes in the presence of oxygen (3). Second, iron can react with byproducts of aerobic metabolism via Fenton reactions and generate damaging hydroxyl radicals (44, 111). One strategy to provide sufficient iron for cellular function while preventing iron toxicity is to down-regulate expression of iron transport systems in iron-replete conditions. In gram-negative bacteria the Fur protein is a global transcriptional regulator that regulates expression of iron acquisition systems (Figure 1) (45, 47). Fur has two domains, an N-terminal DNA binding domain followed by a C-terminal dimerization domain containing a ferrous iron-binding site (90). In iron-replete conditions, a Fur homodimer binds to its corepressor, ferrous iron, inducing a conformational change. The ferri-Fur complex binds to DNA sequences, known as Fur

boxes, in the promoters of iron-regulated genes (18). Fur boxes are often between or overlapping the -35 and -10 sites in promoters of iron-regulated genes and are formed by a 19 base pair palindromic consensus sequence (18). When Fur is bound to a promoter, transcription is blocked. Under iron-limiting conditions, Fur is iron-free and can no longer bind DNA. Transcription of Fur-regulated genes proceeds (26).

To ensure the requirement for iron is met, bacteria encode many different types of iron transporters (Figure 2) (reviewed in (3)). In the presence of oxygen, insoluble ferric iron is available. A common strategy for ferric iron acquisition is production and transport of siderophores. Siderophores are low molecular weight ferric iron chelators synthesized and secreted by bacteria to obtain iron from the environment (82). Siderophore-bound iron is transported across the outer membrane by specific outer membrane receptors. Transport across the outer membrane requires energy transduction from the cytoplasmic membrane by the TonB-ExbB-ExbD system (52, 92, 94). In the periplasm, a periplasmic binding protein (PBP) delivers the ferri-siderophore to an inner membrane (IM) ATP-binding cassette (ABC) transporter for transport across the inner membrane (70, 98). Free ferric iron can also be transported into the cell by TonB-independent metal ABC transport systems consisting of periplasmic binding proteins and inner membrane ABC transporters (3). It is not clear how free ferric iron reaches the periplasm due to its insolubility in the presence of oxygen (3).

In reducing or anaerobic environments, soluble ferrous iron is available and is thought to enter the periplasm through general porins in the outer membrane (86). Inner

membrane transporters are required for transport into the cytosol. The next section discusses common ferrous iron transporters.

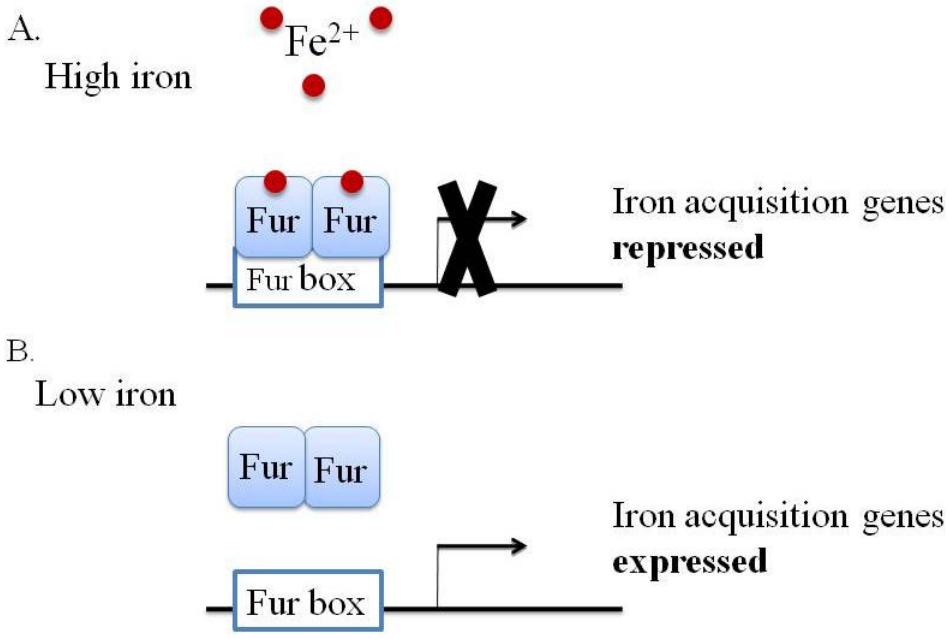

Figure 1. Fur regulation of iron acquisition genes.

(A) In iron-replete conditions a ferri-Fur dimer binds to Fur boxes found overlapping or between the -35 and -10 sites in the promoters of iron acquisition genes. Binding of Fur to Fur boxes blocks transcription of iron uptake genes. (B) When iron is limiting, apo-Fur is no longer able to bind to DNA, and transcription of iron acquisition genes proceeds.

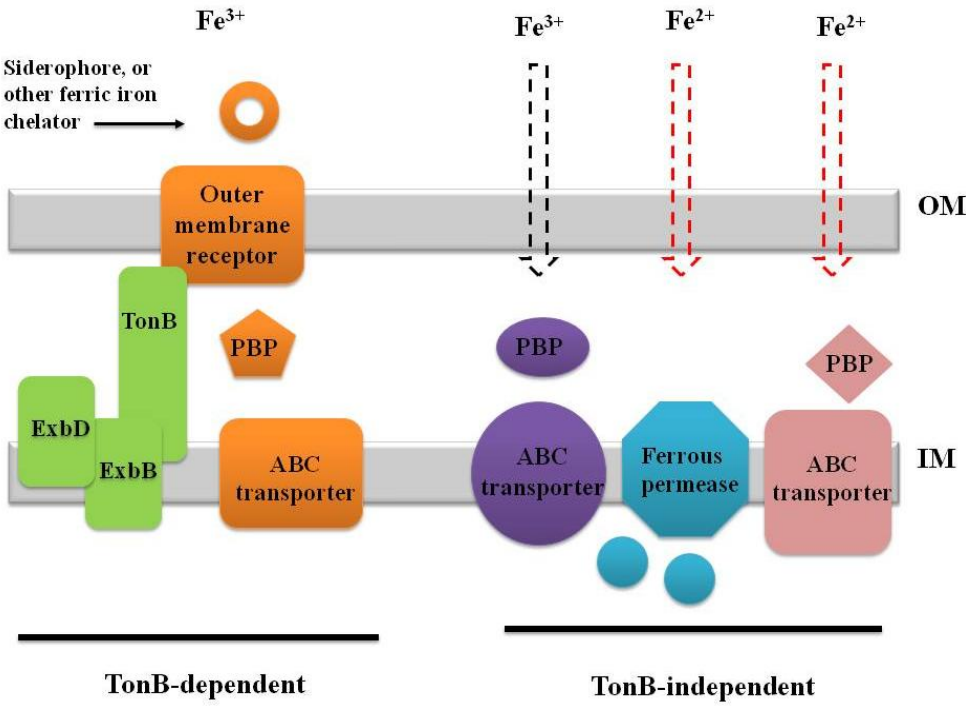

Figure 2. Types of bacterial iron transport systems.

General strategies for iron uptake by gram-negative bacteria are shown and can be divided into two categories based on the requirement for TonB. The TonB-dependent systems are shown on the left. In these systems, siderophores secreted by the bacterium chelate extracellular ferric iron. Ferri-siderophores are transported across the outer membrane (OM) by specific OM receptors and require the TonB system for energy. In the periplasm, a periplasmic binding protein (PBP) delivers the ferri-siderophore to an inner membrane (IM) ATP-binding cassette (ABC) transporter. On the right are TonB-independent transport systems. Ferric iron in the periplasm can be delivered to an inner membrane ABC transporter by a PBP. Ferrous iron can be transported across the inner membrane by IM ferrous permeases or by PBP to an IM ABC transporter specific for ferrous iron.

2. Ferrous iron uptake

In addition to ferric iron transporters, bacteria encode ferrous permeases. Ferrous iron is available in anaerobic and reducing environments (36). Bacterial ferrous iron transporters include the EfeUOB system (42), MntH, (63, 71) the Sit system (64, 120), ZupT (39, 40), and Feo (46, 58). These ferrous permeases are quite different in structure from each other.

EfeU was initially identified in *Escherichia coli* as homolog to the yeast high affinity ferric iron transporter Ftr1p (42) and the Efe iron transport system belongs to a family of transporters known as oxidase-dependent Fe(II) transporters (OFeT). The operon contains three genes, *efeU, efeO,* and *efeB*, and all three genes are required for ferrous iron uptake (19). The functions of the Efe proteins and the mechanism for iron transport remain to be determined. Predicted functions for the Efe proteins have been made based on homology. EfeB is a predicted periplasmic heme-peroxidase and could have a redox function in transport (19). EfeO is a periplasmic protein containing a cupredoxin-like N-terminal domain and may shuttle iron in the periplasm (19). EfeU is predicted to be the cytoplasmic membrane permease (42). The EfeUOB system appears to function best aerobically at low pH as determined by transcriptional fusion studies (19).

The integral membrane protein MntH is homologous to eukaryotic NRAMP (natural-resistance-associated macrophage protein) proteins that transport both iron and

manganese (71). MntH has been shown to transport Mn^{2+} and Fe^{2+} into the cell in a proton-dependent manner (71). MntH has greater affinity for Mn^{2+} and so is characterized as a Mn^{2+} transporter.

The SitABCD proteins have homology to periplasmic-binding protein dependent ABC transport systems used to transport iron-loaded siderophores described in Section 1 (99, 120). The *Salmonella enterica* serovar Typhimurium Sit system has been shown to transport manganese and ferrous iron, but the affinity for ferrous iron is low (64). In contrast, the *Shigella flexneri sitABCD* operon is important for ferrous iron uptake (34).

E. coli ZupT belongs to the ZIP (ZRT, IRT-like) family of metal permeases originally described in eukaryotes. Members of this family often transport multiple ligands (40). ZupT is characterized as a Zn^{2+} transporter, but will also transport Fe^{2+}, Co^{2+}, Mn^{2+} (39), and Cd^{2+} (109). The mechanism for transport is currently not understood, but proton motive force may be required (109). The protonophores carbonyl cyanide m-cholorphenyl hydrazone (CCCP) and carbonyl cyanide-*p*-trifluorometoxyphenyl hydrazone (FCCP), which disrupt proton motive force by allowing protons to cross the bacterial inner membrane (53) inhibit metal uptake by ZupT (109).

3. Feo: a widespread ferrous iron transporter

The first described bacterial ferrous iron transport system, Feo, was identified in *E. coli* over 20 years ago (46). In *E. coli* the operon encoding this system consists of three genes, *feoA, feoB,* and *feoC* and thus encodes three predicted proteins (Figure 3) (20).

While initial characterization and analysis of Feo was performed in *E. coli*, further analyses into other Feo-encoding organisms show conservation of many features (20). Table I contains information regarding identity between Feo proteins from select organisms.

FeoB is the most extensively characterized protein of the Feo system (58). Structurally, FeoB proteins can be divided into three domains; a soluble N-terminal domain is connected by a spacer domain to a C-terminal integral membrane domain (Figure 3) (73). The C-terminal transmembrane domain consists of 8-12 transmembrane helices, depending on the species (20). Due to the large size and membrane-spanning structure of FeoB, it is thought to function as the ferrous permease for iron uptake in the Feo system (20, 73). The N-terminal region of FeoB contains GTP-binding and hydrolysis motifs (designated G1-G5) homologous to eukaryotic small G proteins such as Ras (73). These G protein motifs are the most highly conserved elements of the Feo system (20). In the GTP-bound state, G proteins bind to and regulate the activity of downstream proteins (107). Traditionally, G proteins accomplish this regulation by cycling between GTP- and GDP-bound states (reviewed in (11)). Binding of GTP and Mg^{2+} activates the G protein. This activation causes two regions, known as switch I and switch II, to change conformations. The switch regions, through interactions with effector proteins, are important for the processing of the guanine nucleotides. Upon hydrolysis of GTP to GDP, the γ-phosphate of GTP and the Mg^{2+} ion are released and the

Table 1. Comparison of Feo proteins

	Percent Identity		
	FeoA	FeoB	FeoC
Escherichia coli	100	100	100
Klebsiella pneumoniae	90	89	71
Yersinia pestis	81	75	58
Vibrio cholerae	40	40	11
Vibrio fischerii	48	43	21
Vibrio harveyi	44	44	12
Vibrio parahemolyticus	45	44	12
Vibrio vulnificus	40	43	13
Streptococcus thermophilus	34	43	15[a]
Thermotoga maritima	42	34	15[b]
Methanococcus jannaschii	15	33	10[c]
Pyrococcus furiousus	21	31	-[d]

Feo protein sequences were obtained from either the National Center for Biotechnology Information (NCBI) using the BLAST program (2) or the Comprehensive Microbial Resource (89). Alignment was performed using Clone Manager 9 software. [a] Locus STER_0655 is predicted to encode a protein of 46 amino acids found immediately downstream and in the same orientation as *feoB*. [b] Locus TM_0052 is predicted to encode a protein of 110 amino acids found immediately downstream and in the same orientation as *feoB*. [c] Locus MJ_0565 is predicted to encode a protein of 147 amino acids found immediately downstream and in the same orientation as *feoB*. [d] There is no downstream locus in the same orientation as *feoB*.

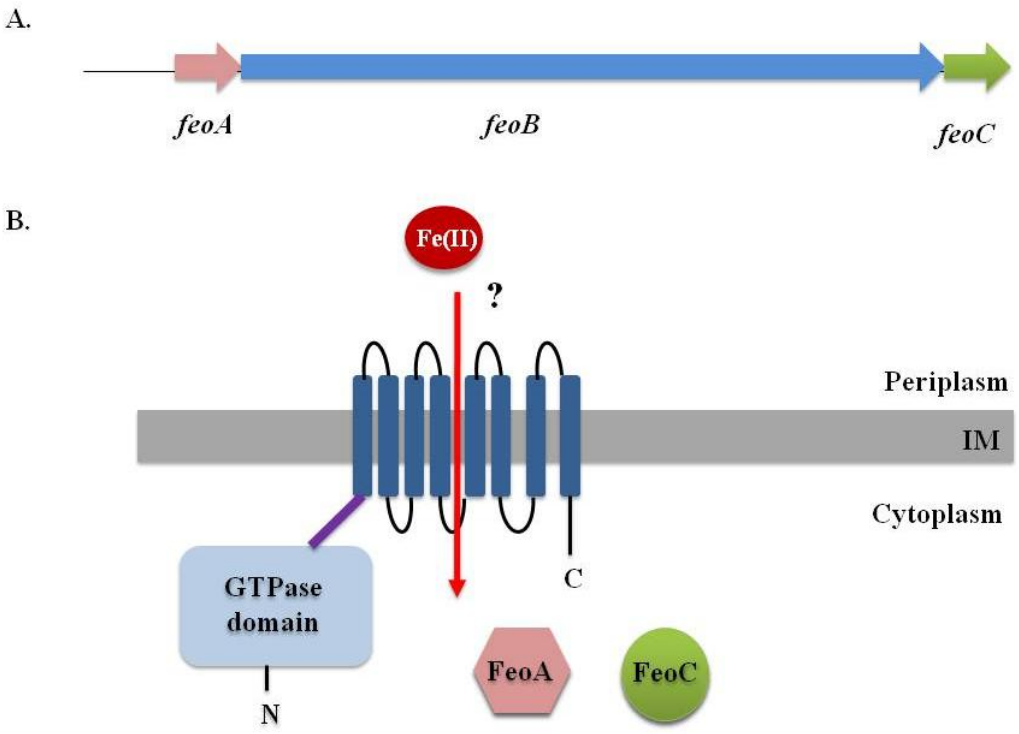

Figure 3. The *feoABC* operon and predicted protein localization.

(A) The *E. coli feoABC* operon. (B) Predicted structure and cellular localization of Feo proteins. FeoB is a large protein with 3 domains; a cytoplasmic, N-terminal, G protein domain (illustrated in light blue), a short spacer domain (in purple), and C-terminal, integral membrane domain (in dark blue). FeoA and FeoC are small proteins of unknown function. Both are predicted to reside in the cytoplasm. Adapted with kind permission from Springer Science+Business Media: Biometals, Feo-Transport of Ferrous Iron into Bacteria, 19, 2006, Cartron, M. L., Maddocks, S., Gillingham, P., Craven, J. C. and S. C. Andrews (20).

conformation of the switch regions changes into an inactive state, thereby inactivating the G protein. GDP then dissociates from the G protein, leaving it in a transient nucleotide-free state which ends when another molecule of GTP binds, allowing the cycle to repeat.

Work by Marlovits, *et al*. (73) first identified the G protein domain of FeoB and demonstrated it is required for iron transport. This work also described FeoB GTPase as having a slow GTP hydrolysis rate and fast GDP dissociation rate. As described above, switch regions of G proteins are important for G protein activity. Mutational studies on the switch regions of *E. coli* FeoB *in vitro* confirmed that these regions are important for nucleotide binding affinity and enzymatic activity (31). *In vivo* studies, these same mutations led to defects in iron transport (31). In this same work, the role of the spacer domain was also examined. The spacer domain, connecting the N-terminal and C-terminal domains of the FeoB protein, is highly variable in sequence (31, 54). The presence of the spacer domain *in cis* to the G protein domain increased the affinity of the G protein domain for a fluorescent GDP analog by approximately 12-fold, but had no effect on either GTP binding affinity or GTPase activity (31). Based on these results, it was proposed that the spacer domain acts as a guanine nucleotide dissociation inhibitor (GDI)-like domain, increasing GDP binding affinity.

Subsequent to the initial studies described above, crystal structures of both the G protein and spacer domains of FeoB from *E. coli* (43), *Thermotoga maritima* (48), *Legionella pneumophila* (88), *Klebsiella pneumoniae* (54), *Pyrococcus furiosus* (54), and *Streptococcus thermophilus* (5) have been published. The crystal structure for the G

protein domain of *Methanococcus jannachii* has also been elucidated (65, 66). Taken together, these structures confirm that the G protein domain of FeoB forms a traditional G protein fold consisting of a 6-7 stranded β-sheet surrounded by 5-6 α-helices (30) (Figure 4). The spacer domain forms a hammer-shaped helical domain (54) consisting of 4-5 smaller α- helices followed by an extended α-helix designated the "valve" helix (43). The folding of the spacer domain has not been seen in other proteins, and therefore could represent a new protein domain (43, 48, 88). Despite the lack of sequence conservation between species, the helical domains of the spacer domain are conserved (54) suggesting that selection has operated on the overall structure of the region, but not the specific protein sequence, and further suggesting that the structure plays an important role in the function of the protein.

A surprising finding from crystal structures of the FeoB G protein and the spacer domains was that the spacer domain and the G protein domain interact at multiple locations across a large interface (5, 48, 54, 88). Some of these interactions involved residues in or near switch II of the G protein domain making contact with residues in the valve helix of the spacer domain (5, 48, 54, 88), which has been proposed to be located near the membrane-embedded C-terminal domain of the FeoB protein (43). Observed structural changes in the helical domain upon GTP binding bring the helical domain closer to switch II and could lead to movement of the valve helix (43). If the suggestion that valve helix is in proximity to the transmembrane domains is correct, this helix could be located in a prime position to regulate ferrous iron translocation through the inner

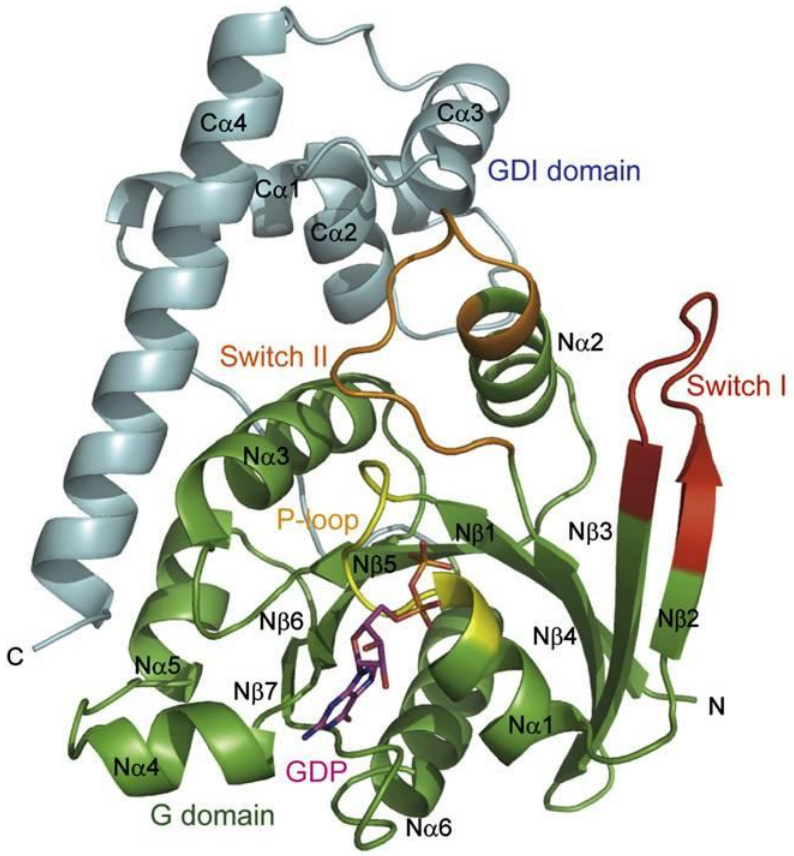

Figure 4. Structure of *Thermotoga maritima* FeoB cytosolic domain bound to GDP.

Ribbon representation of GDP-bound FeoB from *T. maritima*. The G domain is in green, the GDI domain in cyan, the P loop in yellow, switch I in red and switch II in orange. Helix C4α is the proposed "valve" helix. GDP is shown in stick representation. PDB file 3A1S. Reprinted from (48) with permission from Elsevier.

membrane (43, 88). The proposed effector function of the valve helix as a regulator of ferrous iron translocation is based the observed location of the valve helix a single crystal structure lacking the C-terminal membrane domain of FeoB, and so needs to be experimentally tested. Further work is needed to determine if the spacer domain acts as a GDI-like domain increasing GDP binding affinity (31), as an effector domain to regulate ferrous iron translocation (43), or both (48, 54, 88).

Despite the similarities described above, many differences have also been observed when comparing the structures of the FeoB G protein and spacer domains between species, and much remains to be elucidated about the structure and function of the FeoB protein. The switch regions of the FeoB G protein domain are major structural features that are not consistently oriented in crystal structures from different species. In eukaryotic G proteins, switch I is located in proximity to the nucleotide binding site and is stabilized by an interaction with the γ-phosphate of GTP (66). In the *M. jannaschii* (66) and *T. maritima* (48) GTP-bound FeoB crystals, switch I is disordered but points away from the nucleotide binding site. In contrast, the FeoB crystal structure from *S. thermophilus* indicates that switch I forms a lid over the nucleotide, burying all three phosphates (5). Both switch regions are predicted to undergo conformation changes upon GTP hydrolysis (11). In the crystal structures from *M. jannaschii* (66) and *T. maritima* (48) there is no observed conformational change in switch II between the GDP- and GTP-bound FeoB G protein domain crystals while structures from *E. coli* (43) and *S.*

thermophilus (5) indicate that switch II undergoes conformational changes, as expected. Further work will be needed to investigate these discrepancies.

The crystal structures of the FeoB G protein and spacer domain have provided a wealth of information about FeoB. However, it still remains to be shown that FeoB is the ferrous permease for iron transport by Feo. Furthermore, in this body of literature FeoB has been reported as a monomer (5, 48, 88), dimer (54), and a trimer (43, 54). Determining the *in vivo* structure of FeoB is critical to the understanding Feo-mediated iron transport. It has been suggested that a FeoB trimer forms the pore for iron translocation (43), but this remains to be proven.

In addition to gaps in structural knowledge of FeoB, the enzymatic activity of FeoB needs to be further examined. FeoB has been reported to have slow GTP hydrolysis rate (73) and it is not clear if this rate is sufficient to meet the requirement for iron in the cell with assistance from effector proteins. Many G proteins use GAPs, or GTPase-activating proteins, to stimulate hydrolysis of GTP to GDP and deactivate the G protein (9). To date, no GAPs for FeoB have been identified. Recently however, Ash, *et al*. (5) demonstrated a 20-fold acceleration of GTPase activity in the presence of K^+ and identified a critical residue, Asn11, required for this activation. The K^+ did not affect GTP or GDP binding affinity. Further work is needed to determine if this stimulation of FeoB GTPase activity is physiologically relevant to iron transport.

Based on the crystallographic structural data on the FeoB G protein and spacer domain discussed above, a preliminary model of FeoB function is proposed (Figure 5).

The proposed mechanism is as follows (A) FeoB binds GTP and Mg^{2+} leading to conformational changes in both switch I and switch II. (B) Switch I shifts towards the nucleotide-binding site, forming a lid over GTP (5). (C) Switch II and the helical domain become closer to one another. (D) The movement of the helical domain moves the valve helix, which could regulate ferrous iron translocation through the membrane (43). (E) GTP hydrolysis to GDP relaxes the switch regions to their inactive state, the helical domains shift away from switch II and the valve helix returns to its inactive position. While this model does offer an explanation for the mechanism of ferrous iron transport by FeoB, it remains highly speculative as it is based on incomplete and often conflicting data.

Eighty percent of organisms that possess a *feoB* homolog encode *feoA* (20). FeoA is a small 75 amino acid cytoplasmic protein with a predicted high pI (pI=9.43) (20). The function of FeoA is not known. The amino acid sequence of FeoA has weak identity (16%) to the C-terminal region of *Corynebacterium diphtheriae* DtxR (20), a global iron regulator, which is functionally similar to Fur (12). The function of the C-terminal domain of DtxR is not known, but has been noted to contain a SH3-like fold. SH3 domains in eukaryotes are found in signaling and cytoskeletal proteins and often mediate protein-protein interactions (28). The significance of this structural homology is not known.

The last gene in the *E. coli feo* operon is *feoC* (20), which is predicted to encode a 78 amino acid protein, FeoC. FeoC has been proposed to be a transcriptional regulator of

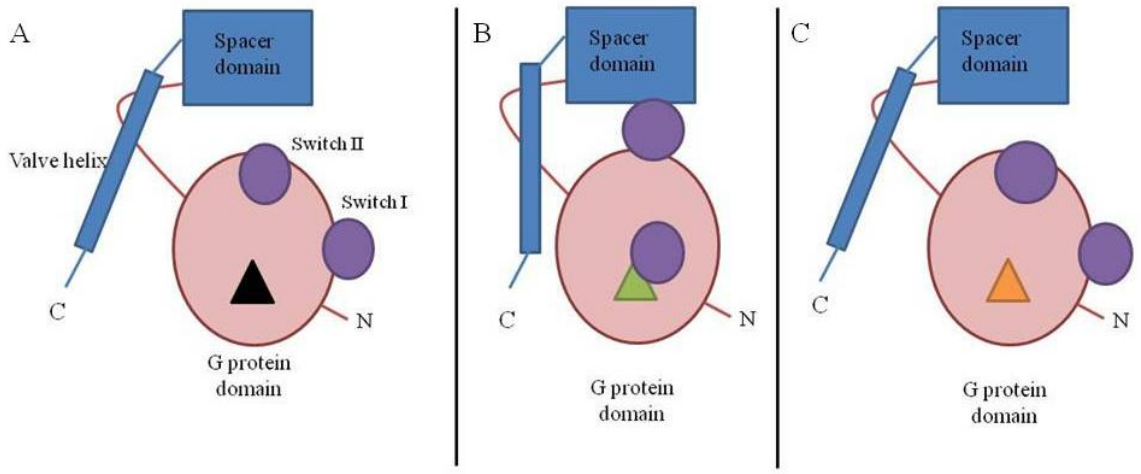

Figure 5. Model for structural changes in FeoB due to GTP hydrolysis.

(A) Transiently, FeoB starts with an empty nucleotide binding site (indicated as a black triangle). (B) Upon GTP and Mg^{2+} binding (illustrated as a green triangle), switch I shifts toward the nucleotide binding site, forming a lid over GTP. Switch II moves closer to the spacer domain leading to movement of the valve helix away from the membrane-embedded portion of FeoB (not shown). (C) GTP hydrolysis to GDP (shown as an orange triangle) relaxes the switch regions and the valve helix returns to its inactive position. GDP will leave the nucleotide binding site and when a molecule of GTP fills the nucleotide binding site, the process will start over.

the *feo* operon based on two observations (3). First, FeoC contains a winged-helix fold, a type of helix-turn-helix (HTH) domain, in its N-terminus. HTH folds are often associated with DNA-binding proteins, including transcriptional regulators (13). Secondly, alignment of numerous FeoC sequences showed conservation of four cysteine residues which are proposed to comprise an [Fe-S]-cluster binding site. Carton *et al*. (20) hypothesized that binding of an [Fe-S]-cluster would cause a structural change in FeoC that could lead to a change in DNA-binding affinity. The role of FeoC as a transcriptional regulator, possibly of the *feo* operon, remains to be experimentally tested.

Three environmental signals have been found to experimentally regulate *feo* expression: 1) iron limitation (47, 58), 2) anaerobiosis (58), and 3) acidic pH (24, 56). Consistent with other iron transport operons, Feo is Fur-regulated (46, 58), leading to increased *feoABC* expression under iron-limiting conditions. Both anaerobiosis and acidity promote ferrous iron availability. It has been demonstrated that *E. coli feo* is induced under anaerobic conditions by FNR (58), a transcription factor that regulates gene expression in response to oxygen. FNR activity requires an [Fe-S] cluster, often promoting expression of genes needed for growth under low oxygen concentrations (67, 68). The *feo* operon has also been shown to be regulated by pH. In *Salmonella enterica* the RstA response regulator binds to the *feo* promoter and induces *feo* expression in low pH in a mechanism that requires the PhoP/PhoQ two-component system (24, 56). It remains to be determined if other conditions regulate *feo* expression, but these two

regulatory mechanisms suggest that *feo* expression is increased under conditions where ferrous iron predominates, consistent with a role for Feo in ferrous iron transport.

Feo is known to be an important *in vivo* iron uptake system for many enteric pathogens, all of which inhabit the gastrointestinal tract, a low oxygen environment. Mutations in *feoB* have been shown to attenuate the virulence of some enteric pathogens such as *E. coli* (58)*, Helicobacter pylori* (113) and *Salmonella typhimurium* (112). In addition, the loss of *feo* has been shown to attenuate non-enteric pathogens including *Legionella pneumophila* (96), *Porphyromonas gingivalis* (29), *Streptococcus suis* (4), and *Xanthomonas orzae* (84) further underscoring the importance of Feo in virulence.

4. Vibrio cholerae

The model organism for our studies of bacterial iron transport is *Vibrio cholerae. V. cholerae* is a curved gram-negative bacterium and the causative agent of cholera, an acute diarrheal illness characterized by "rice water stools." Of over 200 serotypes of *V. cholerae,* currently only two, O1 and O139, are able to cause epidemic and pandemic cholera (33). However, non-O1 and non-O139 strains can cause intestinal and extraintestinal illness on occasion (100, 103).

In the environment, *V. cholerae* is a natural inhabitant of brackish and estuarine water (25), where it lives as a planktonic bacterium or in association with algae (108), zooplankton (108), crustaceans (55) and plants (106). On these surfaces *V. cholerae* forms biofilms (74, 115), multicellular, three-dimensional structures that aid in survival

under stress conditions (121). Cholera is especially problematic in developing nations because of poor sanitation and a lack of clean water. The World Health Organization estimates there are 3-5 million cases of cholera annually, resulting in 100,000-120,000 deaths per year (1).

Ingestion of contaminated water is the most common route of infection. After ingestion, the bacteria must survive passage through the acidic stomach to arrive at the site of colonization, the small intestine. *V. cholerae* pathogenesis is complex and multifactorial, but two virulence factors are essential for infection, cholera toxin (CT) (51) and the toxin co-regulated pilus (TCP) (7, 51, 110). As *V. cholerae* is a non-invasive pathogen TCP is essential for adherence to host intestinal epithelial cells (51). Once established, *V. cholerae* produces CT, an AB subunit toxin, the action of which results in the characteristic symptoms of cholera (59). The pentameric B subunit interacts with the CT receptor, ganglioside GM_1, permitting entry of the A subunit into the cell (27). Once inside, the A subunit targets adenylate cyclase, an important host cell regulator that is responsible for the production of cyclic adenosine monophosphate (cAMP) from ATP (59). CT catalyzes the transfer of an ADP-ribose moiety from nicotinamide adenine dinucleotide (NAD) on to $G_{S\alpha}$ (21, 38), a G protein regulator of adenylate cyclase. ADP-ribosylation of $G_{S\alpha}$ leads to permanent activation of adenylate cyclase, which leads to increased cAMP in the cell. The increase in cAMP causes the cell to increase chloride secretion and decrease sodium chloride absorption resulting in an electrolyte imbalance. In an attempt to correct this imbalance, there is an outpouring of water from the cells,

leading to diarrhea. The watery stools of infected individuals can contain large numbers of highly motile *V. cholerae* (75).

5. *Vibrio cholerae* iron acquisition

Reflecting the importance of iron in the survival and pathogenesis of *V. cholerae*, over 1% of the genome of this pathogen is dedicated to iron acquisition genes (116). These genes are distributed on both *V. cholerae* chromosomes (116). By encoding multiple iron transport systems, *V. cholerae* is able to meet its iron requirements under the varying conditions in each of the ecological niches it occupies.

The catechol siderophore vibriobactin is the sole siderophore produced by *V. cholerae* (41, 85) and is transported by the outer membrane receptor ViuA (16). In addition to receptors for its endogenous siderophore, *V. cholerae* encodes outer membrane receptors for enterobactin (78), a siderophore produced by *E. coli,* and ferrichrome (41), a siderophore produced by some fungi. Vibriobactin and enterobactin can both be transported across the inner membrane by two separately encoded periplasmic binding protein-dependent ABC transporters (118), ViuPDGC (16) and VctPDGC (78), while ferrichrome is transported by the FhuBCD perpiplasmic binding protein-dependent ABC transporter (116). In addition to multiple siderophore-based systems, *V. cholerae* encodes three outer membrane receptors for heme (49, 50, 76). All of these systems use energy provided by the TonB-ExB-ExbD system to transport their respective substrates across the outer membrane. *V. cholerae* has two TonB systems (83) that have both specific and redundant transport functions (102). One interesting

difference between the two TonB proteins is that TonB1 is longer than TonB2 and is predicted to span the periplasm more easily (102). This is expected to be important in environments of high osmolarity, including seawater, where the distance between the inner and outer membrane could be increased (102).

Free ferric iron in the periplasm can be transported into *V. cholerae* by FbpABC (117). FbpA is a periplasmic binding protein that shuttles iron to the inner membrane ABC transporter encoded by *fbpBC*. The mechanism for transport by Fbp or how ferric iron reaches the periplasm is not known, but this system is known to function independent of TonB (117)

The sole ferrous iron transport system of *V. cholerae* is encoded by the *feoABC* operon (117). *V. cholerae* FeoA and FeoB have 40% identity to their *E. coli* homologs (117). Interestingly, the predicted *V. cholerae* FeoC protein has only 11% identity to *E. coli* FeoC. Consistent with other enteric pathogens, *V. cholerae* Feo could be an important iron acquisition system during infection. Microarray analysis has shown that the *feo* genes are among the most highly expressed in the gastrointestinal environment in vibrios collected from a rabbit ileal loop model of infection (119) and in stools from cholera patients (8). The mechanism of Feo-mediated iron transport is not known.

In addition to ferrous and ferric iron transport systems, *V. cholerae* encodes the novel iron utilization protein VciB (77). Present in few organisms, VciB was originally identified in a screen for genes which stimulate the growth of an *E. coli* siderophore synthesis mutant and is predicted to encode a cytoplasmic membrane protein that

contains three transmembrane helices and a large periplasmic loop. Work by Mey *et al*. (77), demonstrated that growth stimulation by VciB required a functional ferrous iron transport system and was TonB-independent. The mechanism by which VciB promotes iron uptake remains to be determined.

Despite all that is known about iron transport in *V. cholerae,* much remains to be discovered. *V. cholerae* containing mutations in *fbpA*, *feoB*, and *vibB* (a siderophore biosynthesis gene) still forms colonies, indicating at least one iron transport system remains to be identified (117). Additionally, little is known about the Feo ferrous iron acquisition system, the sole ferrous iron transport system characterized in *V. cholerae*.

6. Purpose of this research

feo operons have been described in archaea (54, 65, 66) and in many diverse bacteria, including gram-negatives (46, 54, 88, 117), gram-positives (4, 5, 57), spirochetes (69), and cyanobacteria (23, 62). Despite the wide distribution of the *feo* operon and over 20 years of study, the mechanism of ferrous iron uptake by Feo is not understood. While FeoB is presumed to be a ferrous permease, this has not been shown experimentally. Additionally, the roles of the products of the other two genes in the *feo* operon, *feoA* and *feoC*, remain to be elucidated. The purpose of this research project is to characterize the *V. cholerae feoABC* operon and the gene products it encodes. This study will advance our understanding not only of the Feo system in *V. cholerae*, but of ferrous iron acquisition in a wide range of organisms across two domains of life.

II. MATERIALS AND METHODS

1. Bacterial Strains and Plasmids

Bacterial strains used in this study are listed in Table 2. Bacterial plasmids used in this study are listed in Table 3. *E. coli* DH5α was used for routine cloning procedures. *E. coli* RS5033 was used when cloning with restriction enzymes that are sensitive to DNA methylation by *dam* methylase. Plasmid pTAP403 was a gift from Dr. Scott Stevens, University of Texas, Austin.

2. Media, Reagents, and Growth Conditions

Bacterial strain stocks were maintained in tryptic soy broth (TSB) plus 20 % glycerol at -80^{O}C. *E. coli* strains were grown in Luria-Bertani (LB) broth (1% tryptone, 0.5% yeast extract, 1% sodium chloride) or on LB agar. *Shigella flexneri* SM193w was grown in LB broth or on LB agar plates supplemented with siderophore-containing supernatant, as described previously (99, 117). When indicated, T-medium (105) was used without added iron and supplemented with 0.2% glucose or sucrose as a carbon source. EZ rich defined medium (EZ-RDM, www.genome.wisc.edu/resources/protocols/ezmedium.html), a modification of supplemented MOPS minimal media described by Neidhardt (80) was used where indicated and was supplemented with 0.2% sucrose.

Media were supplemented with iron as ferrous sulfate ($FeSO_4$) at a final concentration of 100 μM. To chelate iron, ethylenediamine-di-*o*-hydroxyphenyl acetic acid (EDDA) was deferrated as described by Rogers (97), and used at 5 μg per milliliter.

For strains carrying one plasmid, antibiotics were used at the following concentrations per milliliter: 25 μg ampicillin, 25 μg tetracycline, and 50 μg kanamycin. Antibiotic concentrations for *E. coli* H1771 carrying two plasmids were 12.5 μg ampicillin per milliliter and 6.25 μg tetracycline per milliliter.

E. coli BTH101, the host for two-hybrid constructs, was routinely grown at 30^{O}C. To induce expression of two-hybrid constructs isopropyl β-D-1-thiogalactopyranoside (IPTG) was added at a final concentration of 0.5 mM. When BTH101 was grown on LB agar, bromo-chloro-indolyl-galactopyranoside (X-gal) was used at a concentration of 40 μg per milliliter and IPTG was used at a final concentration of 0.5 mM. Antibiotics for BTH101 were used at 25 μg ampicillin and 50 μg kanamycin per milliliter.

Table 2. Bacterial strains used in this study

Strain	Relevant Characteristics	Reference or source
E. coli strains		
DH5α	*endA1, hsdR17, supE44, thi-1, recA1, gyrA, relA1, Δ(lacZYA-argF), U169, deoR [Φ80*d*lacΔ(lacZ)M15]*	(101)
ARM114	W3110 *entF::cam, feoB::kan*	A. R. Mey, Univ. B. Texas, Austin
RS5033	HfrH, *dam-4, ΔlacMS286, phi*80*d*II *lacBK1*thi Str^R	(72)
H1771	MC4100 *aroB, feoB7, fhuF::λplac* Mu	(46, 58)
BTH101	F^-, *cya-99, araD139, galE15, galK16, rpsL1* (Str^r), *hsdR2, mcrA1, mcrB1*	Euromedex
S. flexneri strain		
SM193w	Avirulent SM100 *iuc*::Tn5, *feo*::*tmp, sitA*::*cam*	(117)
V. cholerae strains		
N16961-F	El Tor biotype	R. A. Finkelstein
SAC500	N16961 *lacZ*::*kan*	S. A. Craig, A. R. Mey, Univ. Texas, Austin
Lou15	El Tor biotype	(104)

3. Plasmid DNA Isolation, Restriction Digestion, Gel Extraction of DNA, and Ligations

Plasmid DNA was isolated using GenElute Plasmid Miniprep Kit (Sigma) following manufacturer's instructions and stored at -20^{O}C. DNA was isolated from agarose gels using GenElute Gel Extraction Kit (Sigma). In both protocols, elutions were into sterile Milli-Q (Millipore, Billerica, MA) purified water. Restriction enzyme digestion was performed by following manufacturer's (New England Biolabs) protocols. Ligation of DNA was performed using T4 DNA ligase (New England Biolabs) according to manufacturer's protocol.

To generate blunt ends using DNA polymerase I, 1 unit of Klenow (New England Biolabs) per μg DNA was placed in 1X Buffer 2 (New England Biolabs) and 40 μM each dNTP and incubated for 15 minutes at 25^{O}C. The reaction was stopped by adding ethylenediaminetetraacetic acid (EDTA) at a final concentration of 10 mM. The enzyme was then heat inactivated at 65^{O}C for 10 minutes prior to using the product in a ligation reaction as described above.

DNA molecular weight markers were purchased from New England Biolabs and included ϕX174 DNA-Hae III digest and lambda DNA-BstE II digest.

Table 3. Plasmids used in this study

Plasmid	Relevant Characteristics	Source
pWKS30	Low-copy-number cloning vector	(114)
pACYC184	Low-copy-number cloning vector	(22)
pGEM-T easy	High-copy-number cloning vector	Promega
pQF50	Transcriptional fusion vector carrying a promoterless *lacZ*	(32)
pKT25	Low-copy-number vector encoding T25 under control of *lac* promoter, MCS at 3'end of T25	Euromedex
pKNT25	Low-copy-number vector encoding T25 under control of *lac* promoter, MCS at 5'end of T25	Euromedex
pUT18	High-copy-number vector encoding T18 under control of *lac* promoter, MCS at 5' end of T18	Euromedex
pUT18C	High-copy-number of vector encoding T18 under control of *lac* promoter, MCS at 3' end of T18	Euromedex
pTAP403	Vector for C-terminally TAP tagging proteins	S. Stevens, Univ. Texas, Austin
pFeo101	pWKS30 carrying *V. cholerae feoABC*	(117)
pFeo203	pFeo101 with a frameshift in *feoC*	This study
pFeo204	pFeo101 with a premature stop codon in *feoC*	This study
pFeoΔA	pFeo101 with an in-frame deletion in *feoA*	This study
pFeoBΔG4	pFeo101 with an in-frame deletion in *feoB*	This study
pFeoΔC	pFeo101 with a deletion in *feoC*	This study

Table 3, cont.

pACYCfeoA	pACYC184 carrying *V. cholerae feoA*	This study
pACYCfeoC	pACYC184 carrying *V. cholerae feoC*	C. Fisher, Univ. Texas, Austin
pFeoABC^{TAP}	pFeo101 with C-terminal TAP tag on *feoC*	This study
pKT25-zip	pKT25 carrying leucine zipper of GCN4	Euromedex
pUT18C-zip	pUT18C carrying leucine zipper of GCN4	Euromedex
pKT25FeoB	pKT25 carrying *V. cholerae feoB*	This study
pKT25FeoB179	pKT25 carrying *V. cholerae feoB*, encoding amino acids 1-179	This study
pKT25FeoB272	pKT25 carrying *V. cholerae feoB*, encoding amino acids 1-272	This study
pKT25FeoB(180-272)	pKT25 carrying *V. cholerae feoB*, encoding amino acids 180-272	This study
pUT18FeoA	pUT18 carrying *V. cholerae feoA*	This study
pUT18CFeoA	pUT18C carrying *V. cholerae feoA*	This study
pKT25FeoA	pKT25 carrying *V. cholerae feoA*	This study
pKNT25FeoA	pKNT25 carrying *V. cholerae feoA*	This study
pUT18FeoC	pUT18 carrying *V. cholerae feoC*	This study
pUT18CFeoC	pUT18C carrying *V. cholerae feoC*	This study
pUT18CFeoC-E29G	pUT18C carrying *V. cholerae feoC* with E29G mutation	This study
pQFeo	pQF50 carrying *V. cholerae feo* intergenic region	This study

4. Transformation of Bacterial Strains

a. Transformation of *E. coli* by Heat Shock

Cells were made competent by diluting overnight cultures 1:100 into 25 mL LB broth plus appropriate antibiotics and growing to mid-log (A_{650}=0.4-0.6). The culture was incubated on ice for 30 minutes. The 25 mL culture was pelleted by centrifugation at 5000 rpm for 10 minutes at 4^{O}C and resuspended in 10 mL cold $CaCl_2$ solution (60 mM $CaCl_2$, 15% glycerol, 10 mM PIPES, pH 7). Centrifugation and resuspension was repeated two times, resuspending in 10 mL and 2 mL $CaCl_2$ solution, respectively. The cells were divided into 150 μL aliquots and stored at -80^{O}C. Heat-shock transformation was accomplished by adding ligation products or plasmid DNA to $CaCl_2$-competent cells and incubating on ice for at least 30 minutes. The cells were then heat-shocked at 42^{O}C for 2 minutes and incubated on ice for 2 minutes. The cells were then added to 850 μL LB broth and incubated at 37^{O}C with shaking for 1 hour prior to plating on LB agar plus appropriate antibiotics.

b. Electroporation into *Shigella flexneri*

Shigella flexneri was made electrocompetent by first diluting an overnight culture 1:100 in 25 mL LB broth and growing to mid-exponential phase (A_{650}=0.4-0.6). The culture was incubated on ice for 30 minutes prior to centrifugation at 7000 rpm for 10 minutes at 4^{O}C. Cells were resuspended in 25 mL ice cold water, and centrifugation was

repeated. Next, the pellet was gently resuspended in 10 mL ice cold water and centrifuged, followed by resuspending in 5 mL ice cold water. After a final centrifugation step, the pellet was resuspended in 200 μL ice cold water plus 10% glycerol. Electroporation of DNA into *S. flexneri* was accomplished using the following settings: 200 Ω, 25 μFD, and 2.5 volts. After electroporation, cells were inoculated in 850 μL LB broth and incubated for 1 hour at 37^{O}C with shaking prior to plating on LB agar plus the appropriate antibiotics.

c. Electroporation into *Vibrio cholerae*

V. cholerae was made electrocompetent by diluting an overnight culture 1:100 in 25 mL LB broth and growing to mid-exponential phase. The culture was incubated on ice for 30 minutes. Cells were pelleted by centrifugation at 5000 rpm for 10 minutes at 4^{O}C. Cells were washed two times in 20 mL cold G buffer (137 mM sucrose, 1mM HEPES, pH 8.0) (83). After washing, the cell pellet was resuspended in 400 μL cold G buffer and transferred to a chilled electroporation cuvette (0.2 cm, Bio-Rad). Plasmid DNA (100 ng) was added immediately before electroporation. Cells were electroporated as described above. Immediately after electroporation, cells were resupended in 800 μL LB broth. Cells were grown for 1 hour at 37^{O}C prior with shaking to plating on LB agar plus appropriate antibiotics.

5. Polymerase Chain Reaction (PCR)

Oligonucletide primers used in this study are listed in Table 4. Primers were designed using Clone Manager software (Sci-Ed Software, Cary, NC) and were obtained from Sigma, Invitrogen, or IDT. Lyophilized primers were resuspended in sterile Milli-Q (Millipore, Billerica, MA) purified water to a final concentration of 100 μM and stored at -20^{O}C. All PCR reactions used in plasmid construction were performed using Platinum Pfx polymerase (Invitrogen) according to the manufacturer's protocol. Sequencing of cloned constructs and PCR products were performed by the DNA Sequencing Facility at the University of Texas Institute for Cellular and Molecular Biology on ABI 3130 and ABI 3730 DNA sequencers.

Error prone PCR (17) of *feoC* was performed as follows. A 100 μL master mix was made as follows: 10 μL of 10X Standard Taq Buffer (100 mM Tris-HC1, pH 8.3, 500 mM KCl, 70 mM $MgCl_2$), 3 μL 10 mM $MnCl_2$, 50 pM each primer, 10 ng template, 0.2 mM dATP and dGTP, 1 mM dTTP and dCTP, 5 U of Taq polymerase (New England Biolabs), sterile water to 100 μL. The master mix was divided into 10 μL aliquots and PCR performed with the following parameters: 94^{O}C for 30 seconds, 55^{O}C for 1 minute, 72^{O}C for 1 minute and repeat for 30 cycles.

Table 4. Oligionucleotide primers used in this study

Primer Name	Primer Sequence (5'-3')*
Feo103	GCGGCACCTTCAAGTTGGAAG
Feo114	TGAAGTCGGGGATTTGACGG
Feo200	TGGCGGCCGCTCTAGAAC
Feo201	CGAGATAAGAGCTCGCGCG
Feo202	CGAGCTCTTATCTCGTAGCGCC
Feo203	AAAACATGGCAGAAGCTGAAGCG
Feo204	CGAGCTCTTGATCTCGTAGCGCC
Feo205	CGAGATCAAGAGCTCGCGCG
Feo214	CGAGTCCGTGAGCGAGGAAG
Feo217	CCATGGGAGCCCATCTCTATTTCATC (NcoI)
FeoB227B	ACTCTAGAGATGAAGTATCAAGTACTCAC (XbaI)
Feo228	TACCCGGGGAATCACGCGACAGATACC (SmaI)
Feo229	AGGTCGACTATGATTTTAAATGAACTCAAAGC (SalI)
Feo230	TAGAATTCGACATAGTCACATTCACAGCAAG (EcoRI)
Feo236	ATGGATCCTCGCCTGCTTGCATTTGTGAC (BamHI)
Feo238	ATACCCGGGCTTTTTCGGTGAATTTATGG (SmaI)
Feo239	ATACCCGGGTAGTGAAGTTCAATCTGC (XmaI)
Feo242	TAGAGGATCCCGTTGCTGAATTTGAGTC (BamHI)
FeoA103	CTATGAAATTGTCAGAGAGAGCACAATG
FeoA104	TTGTGCTCTCTCTGACAATTTCATAGAGG
FeoB104	CGGTAAACGAGCACCACAAG
FeoB109	GTTCGCGCTTCACATCCGCAGGATGC
FeoB110	CTGCGGATGTGAAGCGCGAACGTGTTC
FeoC1579	CTCCATGGCTCCGTTTATG (NcoI)
FeoC2632	CTGATTCATGACGCTCTTGTCTCGTAGC
FeoC2772	CGAGACAAGAGCGTCATGAATCAGG

Table 4, cont.

FeoCp4	CATTGGAAAACGTTCTTCGG
FeoTAP2	GTTGGAAGGGATCCCATAGTCACATTC (BamHI)
Rev2	GGAAACAGCTATGACCATG
TAP101	TTATGCTTCCGGCTCCTATG
TAP104	GGGCGGATCCTCGAGGTCGAC (BamHI)

Real time primers

feoB.for	TCCATGGCTCCGTTTATGTCT
feoB.rev	AAAATGCCGCCGCAAA
feoB probe	TGGTGCTCGTTTACCGGTTTATGCGT
toxR for	CCGAAACGCGGTTACCAA
toxR rev	TCGCGAGCCATCTCTTCTTC
toxR probe	TGATCGCCCGAGTGGAAACGG
dksA-1	GGCGCACTTCCGTCGTATT
dksA-2	CGATCGACTTCATCCCTGAGT
dksA probe	TGGAAGCATGGCGTAAT

*Restriction enzyme (indicated in parentheses) sites underlined

6. Construction of Plasmids

6.1. pFeoΔA

pFeoΔA carries an in-frame deletion in *feoA*. pFeo101, containing *V. cholerae feoABC*, (Wyckoff *et al*. 2006) was used as the template for the initial PCR products from primer pairs Feo214-FeoA104 and FeoA103-FeoB104. The products of these reactions were used as template for a splice overlap PCR reaction using primers Feo214-FeoB104. The resulting splice overlap product and pFeo101 were digested with NcoI and SapI prior to ligation.

6.2. pFeoBΔG4

To construct pFeoBΔG4, which contains an in-frame deletion in *feoB*, primer pairs Rev2-FeoB109 and FeoB110-FeoB104 amplifed products from pFeo101. The products from these reactions were used as template for a splice overlap PCR reaction with primer pair Rev2-FeoB104. The splice overlap product and pFeo101 were digested with NcoI and EcoRI before to ligation.

6.3. pFeoΔC

pFeoΔC, carrying a deletion in *feoC*, was constructed by using primer pairs FeoC1579-FeoC2632 and FeoC2773-FeoCp4 to amplify products from pFeo101. The products from these reactions were used as template for a splice overlap PCR using

primer pair FeoC1579-FeoCp4. The splice overlap product and pFeo101 were digested with restriction enzyme NcoI and NotI. The digestion products were then ligated.

6.4. pFeo203

pFeo203 was constructed by using primer pairs Feo200-Feo201 and Feo202-Feo203 to amplify DNA from pFeo101. The resulting products were used as template in a splice overlap PCR using primer pair Feo200-Feo203. pFeo101 and the splice overlap PCR product were digested with the restriction enzymes NotI and AlwNI and the digested products were ligated.

6.5. pFeo204

To construct pFeo204, pFeo101 was used as a template in PCR reactions with the primer pair Feo200-Feo205 and Feo203-Feo204. The products from these reactions were used as template in a splice overlap PCR with the primer pair Feo200-Feo203. The splice overlap product and pFeo101 were digested with the restriction enzymes NotI and AlwNI before ligating the digestion products.

6.6. pACYCfeoA

pACYCfeoA was constructed by first moving *feoABC* from pFeo101 by restriction enzyme digestion with BamHI and EcoRI to pACYC184 digested with EcoRI and BclI. The resulting plasmid was digested with AvaI and ScaI to remove the region

encoding *feoB* and *feoC*. DNA polymerase I, large (Klenow) fragment (New England Biolabs) was used to generate blunt ends. The blunt-ended plasmid was ligated closed.

6.7. pACYCfeoC

pACYCfeoC was constructed by amplifying *feoC* from *V. cholerae* strain Lou15 with the primer pair Feo114-Feo103. The PCR product was ligated into pGEM-T easy. *feoC* was digested out of pGEM-T easy with the restriction enzyme EcoRI and ligated into pACYC184 digested with EcoRI.

6.8. pFeoABC^{TAP}

To construct pFeoABCTAP, first a BamHI site needed to be put at the 3' end of *feoC* on pFeo101. To do this, pFeo101 was used as a template to amplify with the primer pair Feo203-FeoTAP2. pFeo101 and the PCR product were digested with AlwNI and BamHI prior to ligation. Next the TAP tag was amplified from pTAP403 using the primer pair TAP101 and TAP104. This PCR product and the above ligation product were digest with BamHI and then ligated.

6.9. pKT25FeoB

To construct pKT25FeoB, *feoB* was amplified from pFeo101 using primer pair Feo227B-Feo228. The PCR product and pKT25 were digested with XbaI and SmaI and then ligated.

6.10. pKT25FeoB272

To construct pKT25FeoB272, which contains amino acids 1-272 of FeoB on pKT25, the primer pairs Feo227B and Feo238 were used to amplify DNA from pFeo101. Prior to ligation, the PCR product and pKT25 were digested with XbaI and SmaI.

6.11. pKT25FeoB179

pKT25FeoB179 was constructed by amplifying the sequence encoding the first 179 amino acids of FeoB using the primer pair Feo227B-Feo239 from pFeo101. pKT25 and the PCR product were digested with XbaI and XmaI prior to ligation.

6.12. pKT25FeoB(180-272)

The spacer domain of FeoB, encoded in amino acids 180-272, was amplified from pFeo101 with the primer pair Feo238-Feo242. The PCR product and pKT25 were digested with the restriction enzymes BamHI and SmaI prior to ligating.

6.13. pUT18FeoC

To construct pUT18feoC, pFeo101 was used as a template in a PCR using primer pair Feo229-Feo230. This product was ligated into pGEM-T easy. *feoC* was digested out of pGEM-T easy using restriction enzymes SalI and EcoRI. The *feoC* digestion product was ligated into pUT18, digested with SalI and EcoRI.

6.14. pUT18CFeoC

pUT18CfeoC was constructed in the same way as pUT18CfeoC, except the final ligation was into pUT18C digested with SalI and EcoRI.

6.15. pUT18CFeoC-E29G

pUT18CFeoC-E29G was made by performing error prone PCR to amplify *feoC* using primer pair Feo229-Feo230. pUT18C and the randomly mutagenized *feoC* were digested with SalI and EcoRI before ligation.

6.16. pQFeo

pQFeo was constructed by amplifying the *feo* promoter from N16961-F using the primer pair Feo217-Feo236. The PCR product and pQF50 were digested with NcoI and BamHI prior to ligation.

7. β-galactosidase Assays

E. coli H1771 was grown by diluting overnight cultures 1:100 into LB broth plus 100 μM $FeSO_4$ and into LB broth plus 5 μg per milliliter EDDA and growing for 3.5 hours at 37^{O}C. At 3.5 hours β-galactosidase assays were performed as described by Miller (79).

Bacterial adenylate cyclase two-hybrid β-galactosidase assays were performed as follows. A single colony from a plate was used to inoculate a three milliliter culture of LB broth containing 0.5 mM IPTG, 25 μg per milliliter ampicillan, and 50 μg per

milliliter kanamycin. After 24 hours of growth at 30^{O}C with aeration, β-galactosidase assays were performed as described by Miller (79).

8. RNA Isolation and Real Time PCR

E. coli H1771 was grown by diluting cultures 1:50 into LB broth plus 100 μM $FeSO_4$ and growing for 4 hours statically at 37^{O}C. Approximately $4x10^8$ cells were used for RNA isolation. One-fifth volume of 95% ethanol-5% phenol (vol/vol) was added to cultures prior to RNA isolation. Total RNA was isolated using RNeasy Mini Kit (Qiagen) according to manufacturer's instructions. RNA was treated with DNase I (Qiagen) on the RNeasy Mini Kit column and treated with DNase I (Invitrogen) after elution from the column per manufacturers' instructions. RNA samples were ethanol precipitated overnight. Samples were washed twice in 70% ethanol and resuspended in 40 μl diethyl pyrocarbonate (DEPC)-treated water. RNA concentration was quantified on an ND-1000 spectrophotometer (NanoDrop, Wilmington, DE). Using the High Capacity cDNA Reverse Transcription Kit (Applied Biosystems), cDNA was made from 2 μg RNA. Real Time RT-PCR reactions were set up using the TaqMan Universal PCR Master Mix (Applied Biosystems) using 2.5 μL of cDNA diluted 1:10 into DEPC-treated water. Minor groove binding (MGB) primers and 6-carboxyfluroscein (FAM)-labeled probes were designed using Primer Express. The real time reaction was performed on a 7300 real time PCR system (Applied Biosystems) under standard conditions. H1771 samples were normalized to *dksA* control probe. Real time primers and probe sequences are listed in Table 4.

To determine the effect of anaerobiosis on *feo* expression, an overnight culture of N16961-F in EZ-RDM plus 0.2% sucrose plus 2.5 μM ferrous sulfate was diluted 1:100 into EZ-RDM plus 0.2% sucrose. The culture was grown for 2.5 hours at 37^{O}C with aeration before splitting into two cultures. One culture was returned to aerobic conditions while the other culture was placed into an Oxoid anaerobic jar at 37^{O}C. Anaero*Gen* (Oxoid) packets and The Anaerobic Indicator (Oxoid) were used to generate and monitor anaerobic conditions. Both cultures were incubated for one hour before adding one-fifth volume 95% ethanol-5% phenol (vol/vol) to $8x10^{8}$ cells and isolating RNA as described above. cDNA synthesis and real time PCR was set up as described above. N16961-F samples were normalized to a *toxR* control probe. Real time primers and probe sequences are listed in Table 4.

9. In Vivo Crosslinking

An overnight *E. coli* ARM114 carrying pFeoABC^{TAP} was diluted 1:25 into minimal T medium plus 0.2% glucose and grown to mid-log phase. Cells were washed two times in phosphate-buffered saline (PBS) (0.1 M phosphate, 0.15 M NaCl, pH 7.2). Dithiobis(succinimidylpropionate) (DSP or Lomant's reagent) (Pierce, Rockford, IL) was added at a final concentration of 0.5 mM. Samples were incubated for 15 minutes at room temperature with aeration. To stop the crosslinking reaction, Tris, pH 7.5 was added at a final concentration of 20 mM and incubated for 15 minutes. Following the incubation, $8x10^{8}$ cells were centrifuged and resuspended in sample buffer (10% β-mercaptoethanol (BME), 6% (w/v) sodium dodecyl sulfate (SDS), 20% glycerol, 0.2 mg

per mL bromphenol blue) with or without 10% BME. Samples were boiled for 7 minutes and loaded onto two 10% SDS polyacrylamide gels. After electrophoresis, one gel was stained with Coomassie brilliant blue stain (Bio-Rad) and the other gel used for Western blotting. Proteins were transferred to a 0.45 μM nitrocellulose membrane (Hybond-ECL, GE). Blots were probed with anti-TAP antibody conjugated to HRP (generously provided by Scott Stevens, University of Texas, Austin, Texas). The signal was detected by developing the blot using the Pierce ECL-detection kit.

10. Two-hybrid Immunoblotting

BTH101 was grown in the same way as for β-galactosidase assays, described above. $8x10^8$ cells were centrifuged and resuspended in 200 μL of 5X SDS-PAGE sample buffer. Samples were boiled for 7 minutes and loaded onto a 10% SDS-PAGE gel. After electrophoresis, one gel was stained with Coomassie stain and other gel was used to transfer proteins to a 0.45 μM nitrocellulose membrane. After blocking the membrane for 30 minutes in 5% milk in Tris-buffered saline (TBS)-Tween, the membrane was probed with a 1:500 dilution of mouse anti-CyaA (Santa Cruz Biotech) overnight at 4^OC. The membrane was washed three times, for 5 minutes each, in TBS-Tween. The membrane was then blotted with a goat anti-mouse IgG secondary antibody (Bio-Rad) at a 1:10,000 dilution in 5% milk (in TBS-Tween). Binding of antibody was detected as described above.

11. Biolog Phenotypic Microarrays

SAC500, a Lac- N16961 strain, carrying pQFeo was harvested from an LB agar plate and resuspended in 1 mL inoculating fluid IF-0 (Biolog). The cells were then diluted to $2x10^7$ CFU per mL in 100 mL inoculating fluid IF-0. Twenty five mL of this solution were used for plates PM1 and PM2. Immediately prior to dispensing inoculating fluid into the plate wells, fresh X-gal was added at a final concentration of 1.25 mM. Sodium lactate was added to the remaining 75 mL at a final concentration of 0.4% for plates PM3-PM8. As before, immediately prior to dispensing fluid into wells, X-gal was added at to the inoculating fluid at a final concentration of 1.25 mM. Each well in plates PM1-PM8 contained $2x10^6$ CFU per well. Bacteria in inoculating fluid IF-0 were further diluted into inoculated fluid IF-10a (Biolog) to a final concentration of $1x10^5$ CFU per mL for plates PM9 and PM10. X-gal was added to inoculating fluid as described above. Each well in plates PM9 and PM10 contained $1x10^4$ CFU. The phenotypic microarray plates were incubated at 37^OC for 24 hours. The absorbance at wavelengths 595 and 420 nanometers were read on an Opsys MR plate reader (Dynex).

12. Screening for Loss of FeoB-FeoC Interaction

feoC was randomly mutagenized by error prone PCR as described above. The mutagenized *feoC* was used to reconstruct pUT18CFeoC, as described above. The mutagenized pUT18CFeoC was transformed into BTH101 carrying pKT25FeoB272 by heat shock transformation. Cells were plated on LB agar plus antibiotic plus 0.5 mM IPTG and 40 μg per milliliter X-gal. After 48 hours incubation at 30^OC, white colonies were streaked on the same medium. *feoC* on pUT18CFeoC from white colonies

sequenced. Only strains containing single mutations in *feoC* were kept for further characterization.

III. feoA, *feoB*, AND *feoC* ENCODE ESSENTIAL COMPONENTS OF THE *VIBRIO CHOLERAE* FERROUS IRON TRANSPORT SYSTEM

1. *V. cholerae feoA, feoB,* and *feoC* are required for Feo-mediated iron uptake

Characterization of Feo ferrous iron transport systems has been primarily limited to the G protein domain of FeoB. It has been shown previously that *V. cholerae feoABC* can restore iron transport to *E. coli* and *S. flexneri* iron transport mutants (117). It was observed that a clone containing only *V. cholerae feoAB* was unable to transport iron in these strains (data not shown). To define which genes are required for *V. cholerae* Feo function, in-frame deletions in *feoA* (pFeoΔA) and *feoB* (pFeoBΔG4), and a deletion in *feoC* (pFeoΔC) were individually constructed from a clone known to carry a functional *V. cholerae feoABC* operon (pFeo101). *V. cholerae* has many additional iron transporters that could mask the effect of a single iron transport system, so the ability of these constructs to transport iron was tested in two heterologous strains defective in iron transport.

Shigella flexneri SM193w contains mutations in *feoB, iucD,* and *sitA* (99). These mutations impair ferrous iron uptake and aerobactin synthesis in this strain and therefore, growth of SM193w requires supplementation with a usable iron source such as its endogenous siderophore, aerobactin, or complementation with a functional iron transport system (99, 117). As shown in Figure 6A, the *V. cholerae feoABC* operon (pFeo101) stimulated growth of SM193w in the absence of aerobactin as reported previously (117).

When a deletion is present in any of the *V. cholerae feo* genes, SM193w is unable to grow in the absence of aerobactin. All strains are viable and can grow when the medium is supplemented with aerobactin (Figure 6B). These data indicate that *V. cholerae feoA, feoB,* and *feoC* are all required for Feo-stimulated iron uptake in SM193w.

The second heterologous strain used to test for Feo function is *E. coli* H1771 (46, 58). H1771 possesses mutations in *feoB* and *aroB*. The mutation in *aroB* abolishes synthesis of the siderophore enterobactin (35), thus starving this strain for iron. In addition, this strain has a chromosomal *lacZ* fusion to *fhuF*, a Fur-regulated gene. This fusion serves as a reporter for the relative iron status of the cell. When iron starved, transcription from the *fhuF* promoter leads to the production of LacZ. When these cells are plated on medium containing the chromogenic substrate X-gal, colonies appear blue. When complemented with a functional iron transporter, ferri-Fur binds to Fur boxes in iron-regulated gene promoters, including the *fhuF* promoter fused to *lacZ*, blocking transcription and when plated on medium containing X-gal, H1771 colonies appear white.

H1771 complemented with the *V. cholerae feoABC* operon (pFeo101) has low β-galactosidase activity in the presence of iron (Figure 7) (117). This result indicates that the *V. cholerae feo* operon is functional in this strain and Fur is blocking transcription from iron-regulated promoters. Deletions in *feoA* (pFeoΔA), *feoB* (pFeoBΔG4), or *feoC* (pFeoΔC) result in high β-galactosidase activity in H1771. These data support that *V. cholerae feoA, feoB,* and *feoC* are required for iron transport by Feo. To rule out polar

effects of the *feoA* deletion on *feoB*, the *feoA* deletion was complemented in trans with *feoA*. In this complemented strain, there is low β-galactosidase activity. Similarly, when the strain carrying a deletion in *V. cholerae feoC* was complement in trans with *feoC,* β-galactosidase activity levels were low. Therefore, the lack of iron transport seen with *V. cholerae feoA* or *feoC* mutants is due solely to their respective mutations and not due to an effect on *feoB*.

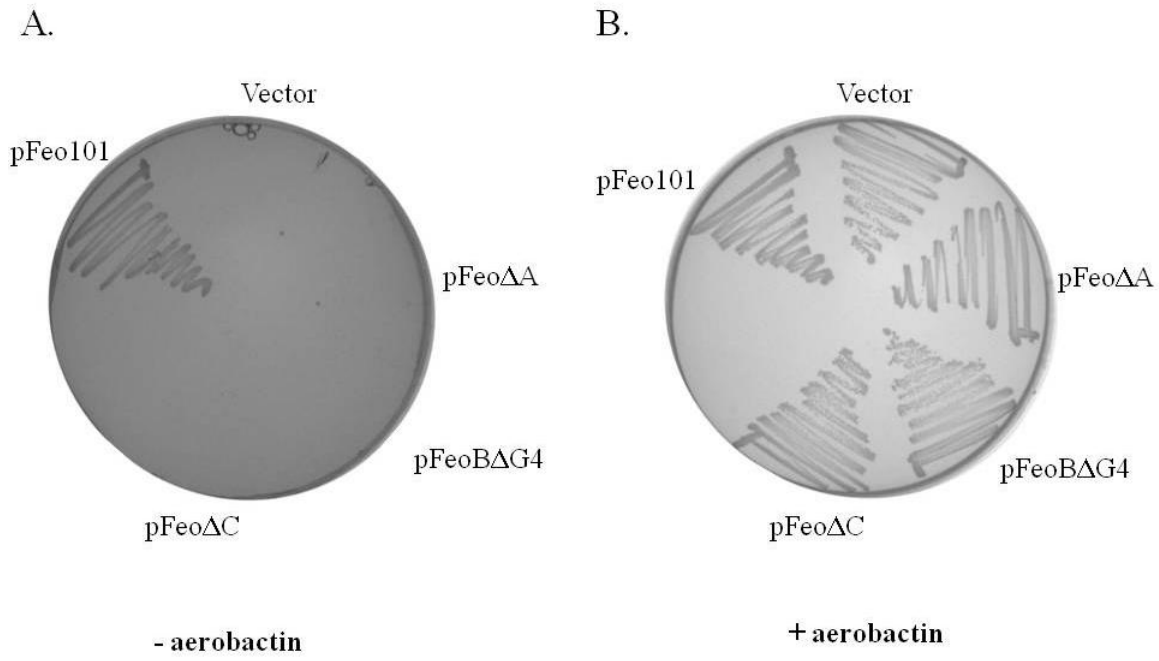

Figure 6. Mutations in *V. cholerae feoA, feoB,* or *feoC* prevent Feo-mediated iron uptake in the iron mutant *S. flexneri* SM193w.

SM193w carrying the empty vector, or plasmids encoding the complete *V. cholerae feoABC* operon (pFeo101), the *V. cholerae feoABC* operon with an in-frame deletion in *feoA* (pFeoΔA), the *V. cholerae feoABC* operon with an in-frame deletion in *feoB* (pFeoBΔG4), or the *V. cholerae feoABC* operon with a deletion in *feoC* (pFeoΔC) were streaked on either (A) LB agar or (B) LB agar supplemented with aerobactin-containing culture supernatant.

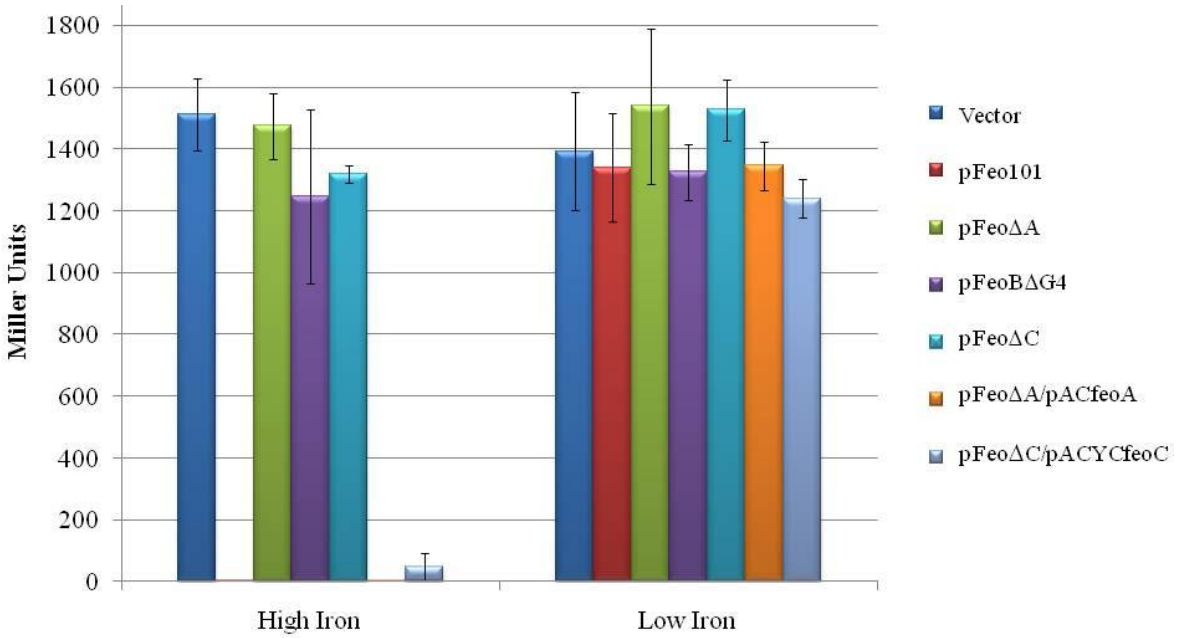

Figure 7. Mutations in *V. cholerae feoA, feoB*, or *feoC* prevent Feo-mediated iron uptake in the iron mutant *E. coli* H1771.

Overnight cultures of H1771 carrying the vector (pWKS30), the complete *V. cholerae feoABC* operon (pFeo101), the *V. cholerae feoABC* operon with an in-frame deletion in *feoA* (pFeoΔA), the *V. cholerae feoABC* operon with an in-frame deletion in *feoB* (pFeoBΔG4), the *V. cholerae feoABC* operon with a deletion in *feoC* (pFeoΔC), the *V. cholerae feoABC* operon with an in-frame deletion in *feoA* (pFeoΔA) complemented with *feoA* (pACYCfeoA), and the *V. cholerae feoABC* operon with a deletion in *feoC* (pFeoΔC) complemented with *feoC (*pACYCfeoC) were diluted into LB broth containing 100 μM $FeSO_4$ (High Iron) or 5 μg per mL EDDA (Low Iron) and grown to mid-log phase. β-galactosidase assays were performed as described by Miller (79). The mean and standard deviation of three independent experiments are shown.

2. *V. cholerae feoC* encodes a protein

In silico analysis of *V. cholerae feoC* did not conclusively indicate that *feoC* encoded a protein. The *feoC* open reading frame is small (228 nucleotides) and the predicted GTG start codon overlaps the *feoB* stop codon. A deletion in *feoC*, however, did abolish iron transport in SM193w (Figure 6A) and in H1771 (Figure 7), demonstrating that this open reading frame is important for Feo function. To investigate why *feoC* is required for Feo function, it was necessary to determine the nature of the *feoC* gene product. There are at least four explanations for a requirement for *feoC* 1) *feoC* could encode a small protein; 2) *feoC* could be part of *feoB,* resulting in a larger FeoBC protein; 3) *feoC* may encode a small RNA; or 4) *feoC* be a cis-acting region with important secondary structure. Different models for *feoC* function can be proposed based on the nature of the *feoC* gene product, so to proceed further it was necessary to define what *feoC* encodes.

To test if *feoC* secondary structure is important either as a region needed *in cis* or as a small RNA, two constructs were made, each containing only a single base-pair change in *feoC*. pFeo203 contains a nucleotide insertion in *feoC* resulting in a frameshift early in the open reading frame. pFeo204 contains a single nucleotide mutation that generates a premature stop codon early in predicted FeoC sequence. The predicted message of wildtype *feoC* and the messages for these mutated *feoC*s were examined using Mfold (122), web-based software for predicting secondary structure of RNA and DNA. No disruption in secondary structure of the *feoC* message was observed in either

feoC containing a frameshift or a premature stop codon (Figure 8). If *feoC* secondary structure were important for Feo function, these mutations are not predicted to affect Feo-mediated iron uptake. These mutated nucleotides are predicted to be found in single-stranded region, and if the fidelity of the sequence is critical for binding to an unidentified target, these mutations could affect *feoC* function.

SM193w was used to test if the secondary structure of *feoC* was important for *V. cholerae* iron transport. The single nucleotide changes in *feoC* that are predicted to disrupt the coding sequence but not secondary structure did not support the growth of SM193w in the absence of aerobactin (Figure 9A). These results led to the hypothesis that either *feoC* encodes a small protein or is part of the FeoB protein. All strains are viable when the medium is supplemented with aerobactin (Figure 9B).

To test if *feoC* encodes either a small FeoC protein or is part of the FeoB protein, a TAP tag (93, 95) was fused in-frame to the C-terminus of *feoC* (pFeoABC^{TAP}). The TAP tag is composed of a calmodulin binding peptide (CBP) separated from Protein A by a tobacco etch virus (TEV) protease cleavage site. The predicted size for FeoC is 8.5 kilodaltons and the TAP tag is approximately 20 kilodaltons, so a FeoC^{TAP} fusion protein would result in a protein of approximately 29 kilodaltons. If *feoC* was part of *feoB*, the tagged protein would be approximately 112 kilodaltons. Western blotting of cells containing pFeoABC^{TAP} with an antibody to the TAP tag clearly shows a TAP-tagged protein of approximately 29 kilodaltons (Figure 10), demonstrating that the *feoC* open reading frame encodes a small protein. No other TAP fusion proteins were observed on the gel.

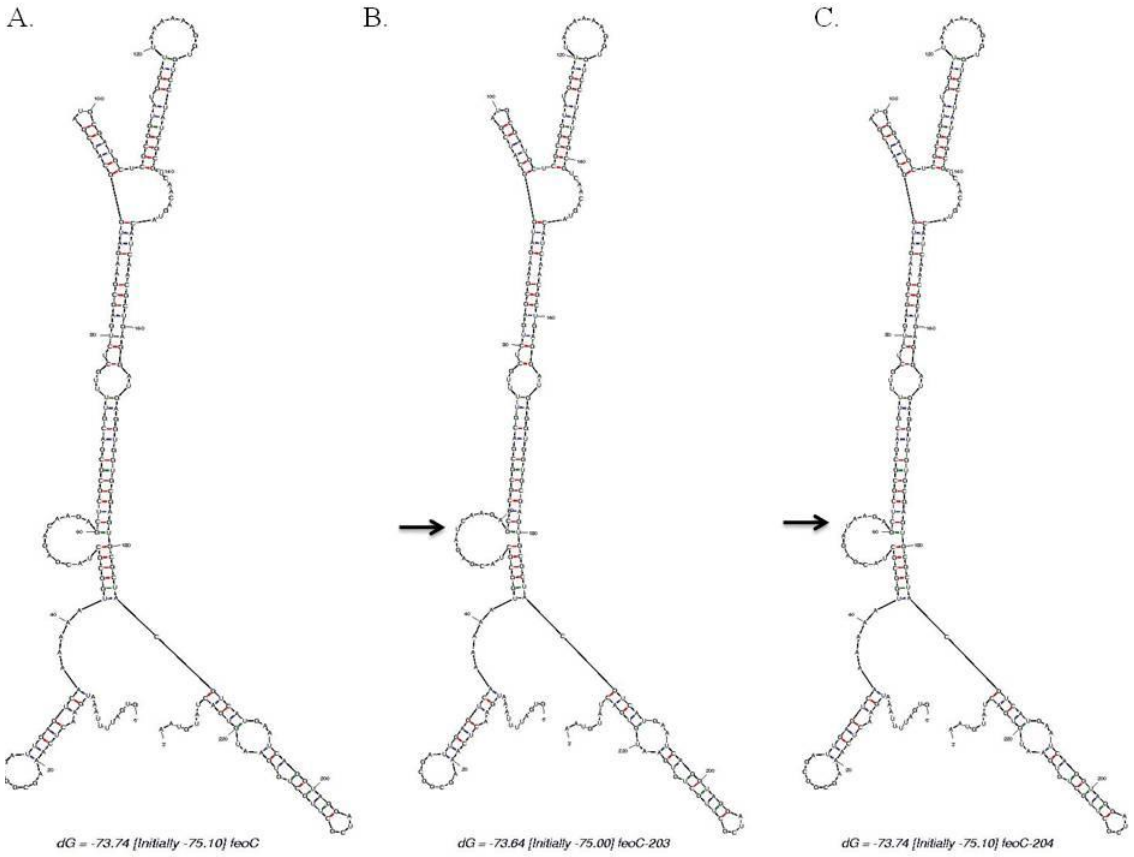

Figure 8. Predicted secondary structure of *feoC*.

Mfold secondary structure predictions of (A) wildtype *feoC*, (B) *feoC* containing a frameshift mutation as designed in pFeo203, and (C) *feoC* containing substitution mutation generating a premature stop codon as designed in pFeo204. The black arrow indicates the position of the mutations in *feoC*. The secondary structure predictions were performed with Mfold (http:/.mfold.rna.albany.edu/?q=mfold) using the default parameters.

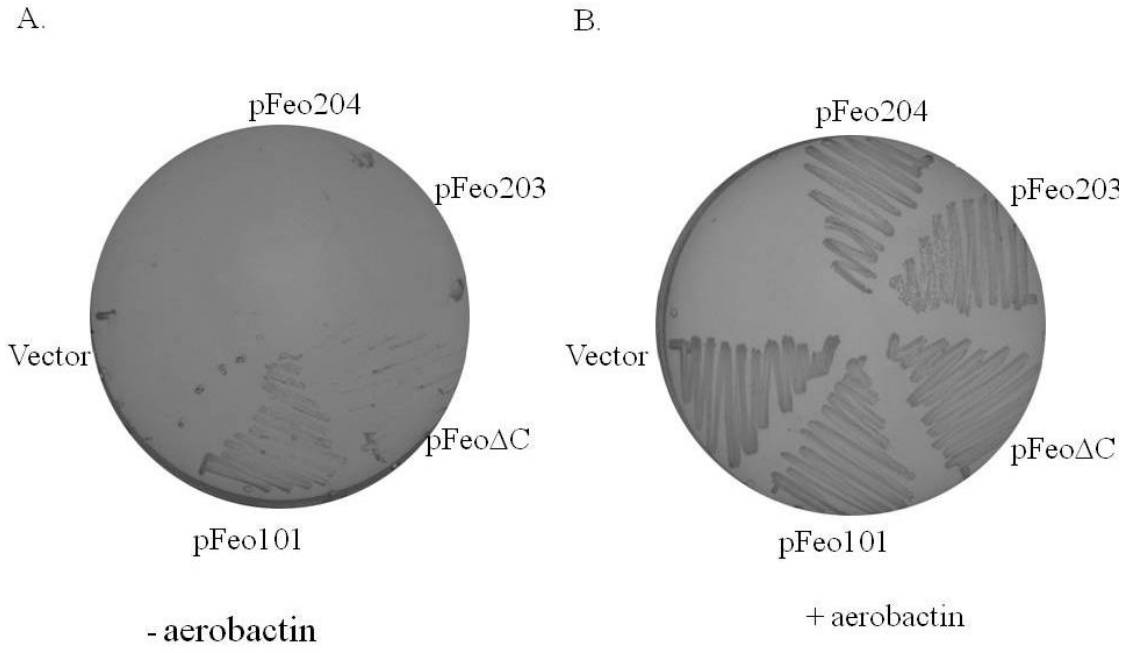

Figure 9. *V. cholerae* Feo containing single nucleotide mutations in *feoC* does not support the growth of the iron mutant *S. flexneri* SM193w.

SM193w containing the empty vector or carrying plasmids encoding the complete *V. cholerae feoABC* operon (pFeo101), *V. cholerae feoABC* operon with a deletion in *feoC* (pFeoΔC), the *V. cholerae feoABC* operon containing a frameshift mutation in *feoC* (pFeo203), and the *V. cholerae feoABC* operon containing a premature stop codon in *feoC* (pFeo204) were streaked on either (A) LB agar or (B) LB agar supplemented with aerobactin-containing culture supernatant.

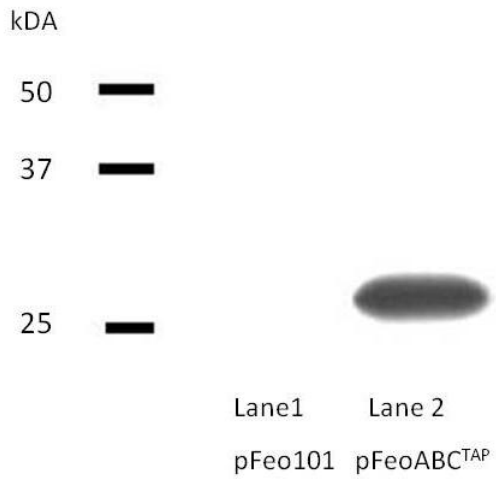

Figure 10. FeoC^{TAP} is a small protein.

Overnight cultures of DH5α containing pFeo101 (the untagged control) or pFeoABC^{TAP} were diluted 1:100 into LB broth and grown to mid-log. Equal numbers of cells were electrophoresed on a 10% SDS-polyacrylamide gel and then transferred to a nitrocellulose membrane. FeoC^{TAP} was detected using a HRP-conjugated antibody to the TAP tag. The estimated size of FeoC^{TAP} is approximately 29 kilodaltons.

A large tag on FeoC could interfere with FeoC function. To determine if *V. cholerae* Feo was functional when a C-terminal TAP tag was placed on FeoC, pFeoABC^{TAP} was tested in H1771 for the ability to repress *lacZ* expression (Figure 11). β-galactosidase activity in H1771 carrying pFeoABC^{TAP} was low, indicating FeoC^{TAP} did not interfere with *V. cholerae* Feo function in *E. coli* H1771.

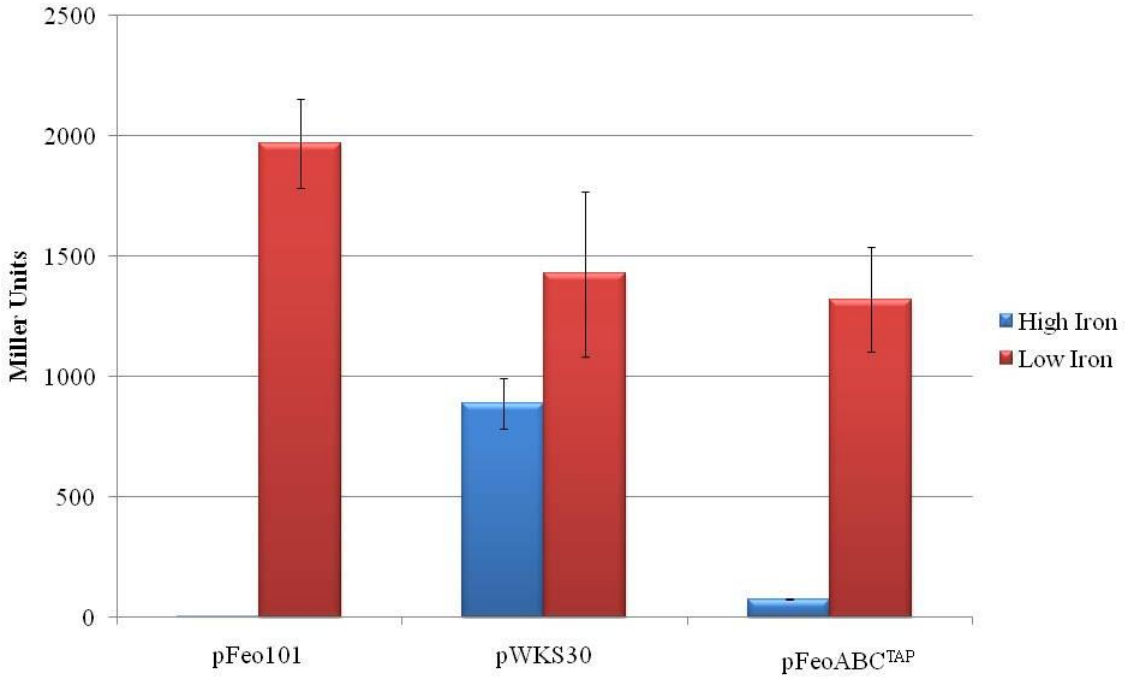

Figure 11. FeoC^{TAP} allows *V. cholerae* Feo to stimulate iron uptake in the iron mutant *E. coli* H1771.

Overnight cultures of H1771 containing the untagged *V. cholerae feoABC operon* (pFeo101), the empty vector (pWKS30), or the *V. cholerae feoABC* operon with a C-terminally tagged *feoC* (pFeoABC^{TAP}) were diluted into LB broth containing 100 μM $FeSO_4$ (High Iron) and 5 μg per mL EDDA (Low Iron) and grown to mid-log phase. β-galactosidase assays were performed as described by Miller (79). The mean and standard deviation of three independent experiments are shown.

3. FeoA and FeoC are not required for expression of FeoB.

FeoA and FeoC are required for Feo-mediated iron uptake but the functions of these proteins are not known. One hypothesis for the requirement of *feoA* or *feoC* is that one or both of these genes is required for expression of the *feo* operon.

To determine if either FeoA or FeoC is required for *feo* expression, *feoB* expression was measured by real time RT-PCR in H1771 strains described in Figure 7. *V. cholerae* has many iron transport systems that could make detecting differences in *feo* expression difficult. In H1771 *V. cholerae* Feo is functional and the relative iron status of the cell can be quantified by measuring β-galactosidase activity. *feoB* mRNA levels, therefore, can be correlated to iron transport in this strain through β-galactosidase assays to determine if either FeoA or FeoC is required for expression of *V. cholerae feo*.

When a deletion is present in *feoA* and iron uptake is impaired (Figure 7), *feoB* is still expressed (Table 5). When the deletion in *feoA* is complemented by *feoA* in trans, *feoB* mRNA levels remain the same (Table 5, compare rows 2 and 3) even though iron transported is restored (Figure 7). In these strains, the *feoB* mRNA levels are decreased as compared to the strain carrying the complete *V. cholerae feo* operon, but these levels of *feoB* expression are sufficient to support iron transport in H1771 (Figure 7). These data indicate the lack of iron transport seen in a strain carrying a deletion in *feoA* is not due to lack of *feoB* expression.

A deletion in *feoC* results in slightly higher *feoB* mRNA levels as compared to a strain carrying the complete *V. cholerae feo* operon (Table 5). Functional complementation of this strain occurs when *feoC* is provided in trans (Figure 7). *feoB* levels remain unchanged between the mutant and complemented strain despite the difference in the ability to transport iron (Table 5, compare rows 5 and 6). Therefore, the lack of iron transport seen in H1771 strains carrying *feoA* or *feoC* mutations is not due to lack of *feoB* expression, and further, neither *feoA* nor *feoC* is required for *feoB* expression.

Table 5. *feoA* and *feoC* are not required for *feoB* expression

	Relative fold change in gene expression	
Relevant genotype	***feoB***	***dksA***
feoA^{+}*B*$^{+}$*C*$^{+}$	1.00 ± 0.00	1.00 ± 0.00
feoA^{-}*B*$^{+}$*C*$^{+}$	0.33 ± 0.03	1.01 ± 0.14
feoA^{-}*B*$^{+}$*C*$^{+}$/*feoA*$^{+}$	0.36 ± 0.03	0.92 ± 0.10
feoA^{+}	0.00 ± 0.00	0.69 ± 0.29
feoA^{+}*B*$^{+}$*C*$^{-}$	1.52 ± 0.40	1.15 ± 0.08
feoA^{+}*B*$^{+}$*C*$^{-}$/*feoC*$^{+}$	1.48 ± 0.22	0.83 ± 0.26
feoC^{+}	0.00 ± 0.00	1.41 ± 0.77

E. coli H1771 carrying plasmids described in Figure 7 was diluted 1:50 into LB broth plus 100 μM $FeSO_4$. Cultures were grown for 4 hours at 37^{O}C statically before isolating RNA. Data shown are the average and standard deviation of three independent experiments. * P-value <0.02, ** P-value <0.0001, determined by an unpaired Student's t-test.

4. FeoC and FeoB interact

The structure of the ferrous iron transporter responsible for Feo-stimulated iron uptake is not known. The Feo proteins may function as a complex, forming a transporter. In this scenario, changes in this complex due to mutations in *feo* genes could abolish iron transport. By identifying any interactions between Feo proteins, insight can be gained into the role that these protein play in iron transport.

Protein crosslinking is a technique commonly used to capture proteins that interact. An *in vivo* crosslinking experiment was performed using the membrane permeable crosslinker dithiobis(succinimidyl)propionate (DSP or Lomant's reagent) in a strain carrying pFeoABC^{TAP}. Protein complexes can then be detected using an antibody to the TAP tag and will be detected by the shift in the migration of FeoC^{TAP}. When a strain carrying pFeoABC^{TAP} is exposed to DSP, a fraction of FeoC^{TAP} migrates slower, indicating higher molecular weight complexes, approximately 125-250 kilodaltons, are formed (Figure 12, lane 2). Protein-protein crosslinkers can be disrupted by the addition of β-mercapatoethanol (BME), and consistent with this, the slower migrating FeoC^{TAP} is not observed following treatment with BME (Figure 12, lane 3). These data suggest that FeoC^{TAP} is interacting with other proteins. The TAP tag is much larger than FeoC, so crosslinking could be occurring with the TAP tag and not with FeoC. For this reason, a second methodology was used to experimentally further test for Feo protein interactions.

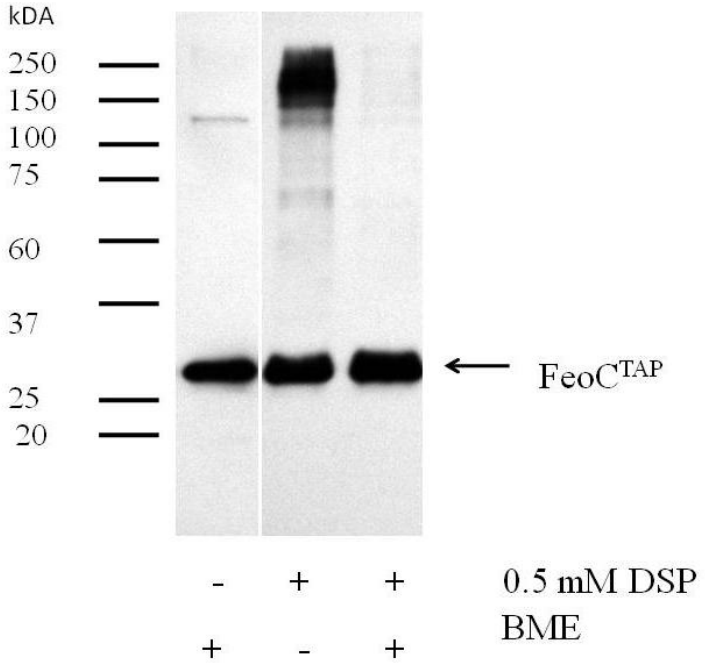

Figure 12. In vivo crosslinking of FeoC^{TAP}.

Overnight cultures of *E. coli* ARM114 (*feoB ent*) were diluted 1:20 in minimal T medium and grown to mid-log phase. Cultures were centrifuged, washed twice, and resuspended in PBS. Proteins were crosslinked with 0.5 mM DSP for 15 minutes. Crosslinking was quenched with 20 mM Tris-Cl, pH 8.0. Equal numbers of cells were centrifuged and resuspended in 5X sample buffer with and without BME. After electrophoresis on 10% a SDS polyacrylamide gel, proteins were transferred to a nitrocellulose membrane. FeoC^{TAP} was detected using an HRP-conjugated antibody to the TAP tag. FeoC^{TAP} encodes a protein of approximately 29 kilodaltons. Lane 1: whole cell lysates in PBS, no DSP, Lane 2: whole cell lysates in PBS, crosslinked with DSP, resuspended in sample buffer without BME, Lane 3: whole cell lysates in PBS, crosslinked with DSP, resuspended in sample buffer with BME.

Bacterial adenylate cyclase two-hybrid analysis (BACTH) is a second method for identifying protein-protein interactions (60, 61). This methodology is based on restoration of adenylate cyclase activity in an *E. coli* adenylate cyclase (*cyaA*) mutant. Two catalytic fragments of *Bordetella pertusiss* adenylate cyclase (T18 and T25) are encoded on separate vectors and are inactive. If two interacting proteins are fused to the catalytic fragments and co-expressed, adenylate cyclase activity is restored and cAMP is synthesized. cAMP, in conjunction with the transcriptional regulator CAP, is a pleiotropic regulator of many genes including the *lac* operon. Screening for interacting proteins can be done by plating on medium containing a chromogenic substrate of LacZ, X-gal. If two proteins interact, colonies will appear blue. Colonies expressing proteins that do not interact will appear white on medium containing X-gal. β-galactosidase assays were performed to confirm the initial screen. This method has been shown to detect interactions among membrane proteins (60), making it an appropriate choice for experiments with FeoB.

BACTH was used to determine if the *V. cholerae* Feo proteins interact. Overexpression of membrane proteins can often be detrimental to the cell, so FeoB was fused to the T25 catalytic fragment, which is encoded on a low-copy-number vector. The N-terminal domain of FeoB is predicted to be cytoplasmic, and therefore the T25 tag was placed on to the N-terminus of FeoB. The cellular location of the C-terminus of FeoB is not known. This T25-FeoB fusion was tested with N- and C-terminally T18-tagged FeoA and FeoC constructs. After screening transformants on medium containing X-gal, β-

galactosidase assays were performed to determine if Feo proteins interact. Commercially provided positive controls have strong β-galactosidase activity when tested, therefore, the manufacturer's established threshold for positive interactions is β-galactosidase activity greater than or equal to 10% of the commercial positive control.

β-galactosidase activity between N-terminally T25-tagged FeoB and C-terminally T18-tagged FeoA did not meet the 10% threshold for β-galactosidase activity for interacting proteins (Figure 13). Moving the T18 tag to the N-terminus of FeoA did not change the low β-galactosidase activity (data not shown). Therefore, there is no detectable interaction between FeoA and FeoB by this method. However, this negative result does not rule out an interaction between FeoB and FeoA.

When N-terminally T25 tagged FeoB was expressed with C-terminally T18 tagged FeoC, a significant increase in β-galactosidase activity as compared to the negative control was observed (Figure 13). The β-galactosidase activity exceeded the activity threshold for interacting proteins revealing that FeoB and FeoC interact. When the N-terminally T25-tagged FeoB was co-expressed with an N-terminally T18-tagged FeoC, β-galactosidase activity is below the 10% threshold for interacting proteins (data not shown). It should be noted that T25-tagged FeoA was also co-expressed with T18-tagged FeoC and no interaction was detected (data not shown).

Interactions between Feo proteins have not been reported. FeoB is a large protein and determining where the FeoB-FeoC interaction occurs could be informative as to the

role of the interaction. FeoB proteins can be divided into three domains: 1) the G protein domain encoded in approximately the first 179 amino acids of *V. cholerae* FeoB, 2) the spacer domain encoded in amino acids 180-272 of *V. cholerae* FeoB, and 3) the transmembrane domains encoded in amino acids 273-758. To determine what portion of FeoB is interacting with FeoC, constructs containing only the G protein domain or the G protein and spacer domains were made. When the N-terminally T25 tagged G protein domain of FeoB (amino acids 1-179) is expressed with either N- or C-terminally tagged FeoC, β-galactosidase activity is low, indicating no interaction between the G protein domain of FeoB and FeoC (Figure 14 and data not shown). However, when an N-terminally tagged construct containing the G protein and spacer domain of FeoB (amino acids 1-272) is co-expressed with a C-terminally tagged FeoC, there is an increase in β-galactosidase activity over the negative control that exceeds the 10% threshold for interacting proteins, showing an interaction between these two proteins (Figure 14). When the T18 tag on FeoC is located on the N-terminus of FeoC, there is a large, significant increase in β-galactosidase activity over both the negative control and the 10% threshold for interacting proteins (Figure 14). These results provide further evidence for an interaction between FeoB and FeoC.

No interaction was detected between FeoC and the G protein domain of FeoB (amino acids 1-179) in this assay. However, if the spacer domain was included with the G protein domain on this construct (FeoB 1-272), the FeoB-FeoC interaction is restored. To determine if the spacer domain of FeoB is sufficient for a detectable interaction with

FeoC, an N-terminal T25 tag was fused to the spacer domain of FeoB (amino acids 180-272). In the presence of either an N- or C-terminally T18-tagged FeoC, β-galactosidase activity is low and did not meet the 10% threshold of activity for interacting results, indicating that the spacer domain of FeoB is not sufficient for an interaction with FeoC in this assay (Figure 15).

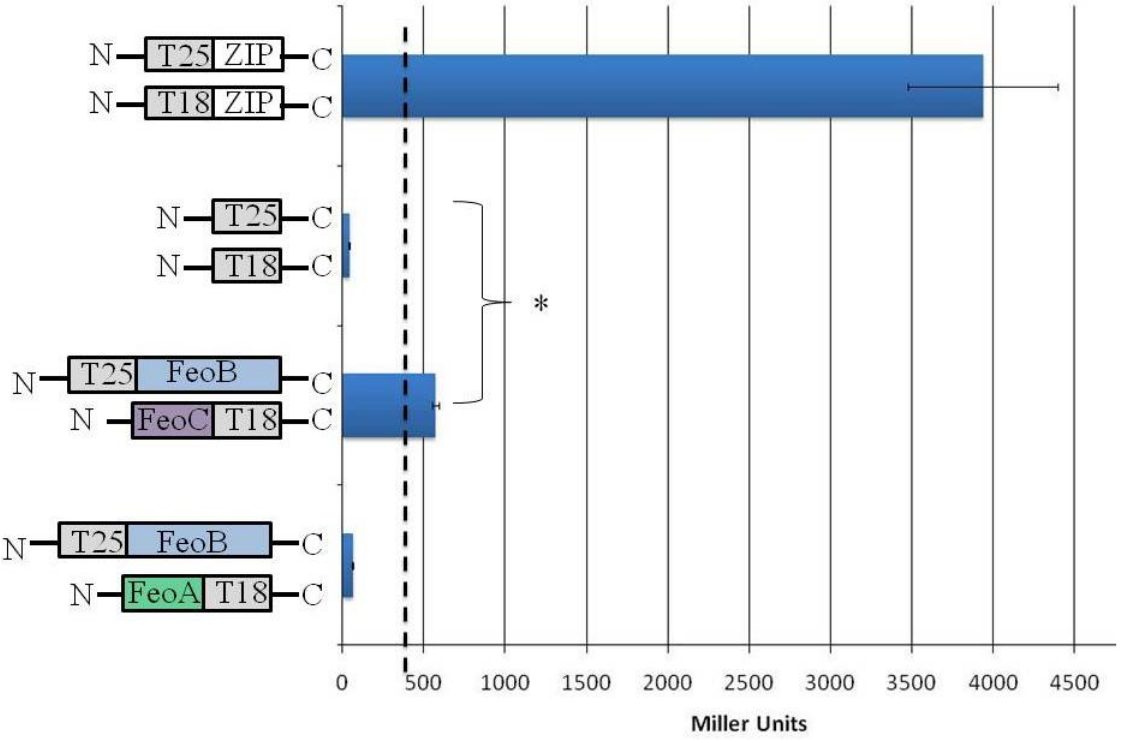

Figure 13. Interactions between *V. cholerae* Feo proteins.

E. coli BTH101 was grown overnight at 30^{O}C in 0.5 mM IPTG before performing a β-galactosidase assay (79). Strains tested are as follows, from top to bottom: BTH101 pKT25-zip pUT18C-zip (positive control), BTH101 pKT25 pUT18C (negative control), BTH101 pKT25FeoB (containing full-length FeoB) pUT18FeoC, BTH101 pKT25FeoB (containing full-length FeoB) pUT18FeoA. β-galactosidase activity is expressed as Miller Units. Vertical dashed line indicates the 10% threshold of positive control. Shown is the average and standard deviation of three independent experiments. * $p<0.0001$, determined by an unpaired Student's t-test.

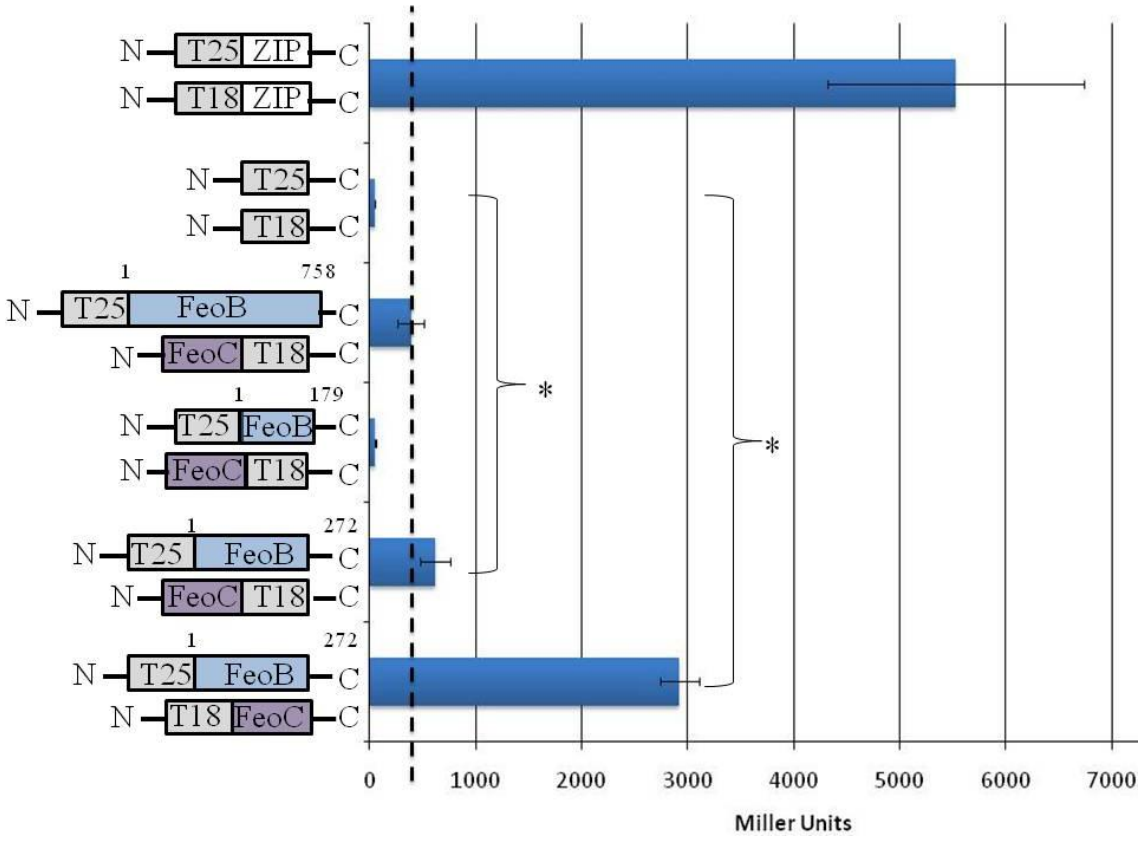

Figure 14. Interactions between *V. cholerae* FeoB and FeoC.

E. coli BTH101 was grown overnight at 30^{O}C in 0.5 mM IPTG before testing β-galactosidase activity (79). Strains tested are as follows, from top to bottom: BTH101 pKT25-zip pUT18C-zip (positive control), BTH101 pKT25 pUT18C (negative control), BTH101 pKT25FeoB pUT18FeoC, BTH101 pKT25FeoB179 pUT18FeoC, BTH101 pKT25FeoB272 pUT18FeoC, and BTH101 pKT25FeoB272 pUT18CFeoC. β-galactosidase activity is expressed in Miller Units. Vertical dashed line indicates 10% threshold of positive control. Shown is the average and standard deviation of three independent experiments. * $p<0.0001$, determined by an unpaired Student's t-test.

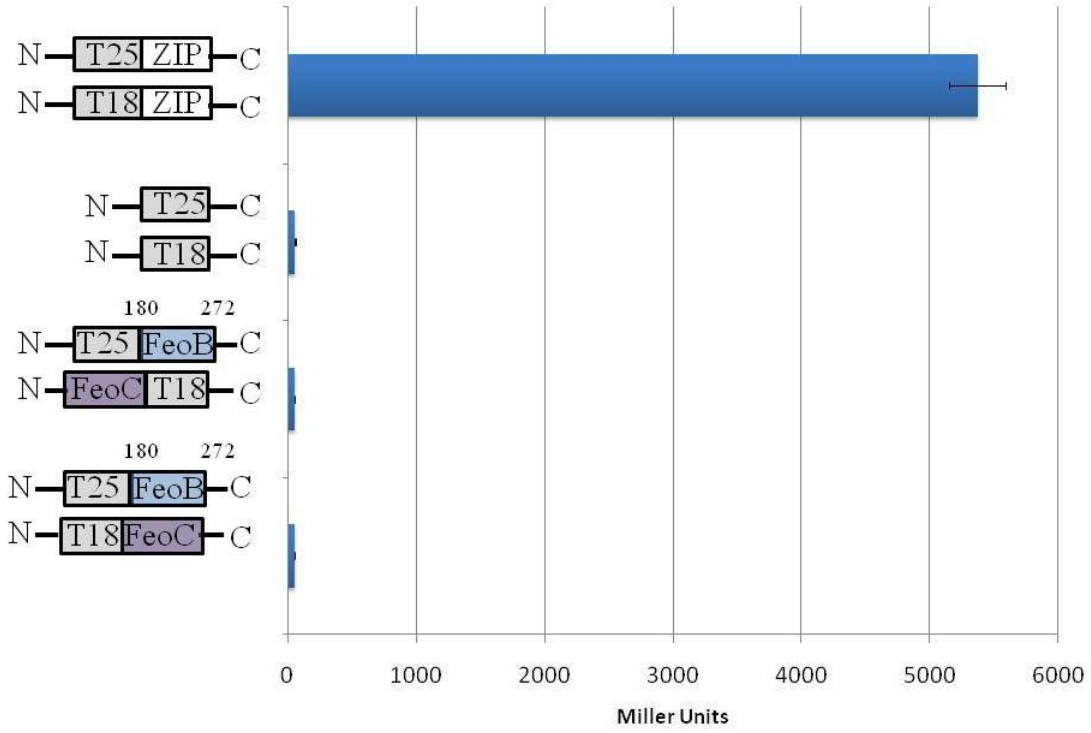

Figure 15. The FeoB spacer domain is not sufficient for the interaction between *V. cholerae* FeoB and FeoC.

E. coli BTH101 was grown overnight at 30^{O}C in 0.5 mM IPTG before performing testing β-galactosidase activity (79). Strains tested are as follows, from top to bottom: BTH101 pKT25-zip pUT18C-zip (positive control), BTH101 pKT25 pUT18C (negative control), BTH101 pKT25FeoB(180-272) pUT18feoC, BTH101 pKT25FeoB(180-272) pUT18CFeoC. β-galactosidase activity is expressed in Miller Units. Shown is the average and standard deviation of three independent experiments.

5. Screening for loss of the interaction between the cytoplasmic domains of FeoB and FeoC

Identifying residues or regions of FeoC that are important for the interaction with FeoB could give insight into the role FeoC plays in ferrous iron transport by Feo. Error prone PCR is one method to randomly generate a large number of different mutations in a given DNA sequence. By combining error prone PCR of *feoC* with BACTH, a method that allows for visual screening, a screen was designed to identify residues in FeoC important for the interaction with the cytoplasmic domains of FeoB. *feoC* was amplified by error prone PCR under conditions optimized to only have one nucleotide mutation per DNA molecule. Mutagenized *feoC* was used to reconstruct the N-terminal T18-tagged FeoC. This construct was transformed into a strain containing the construct encoding the N-terminally T25 tagged FeoB G protein and spacer domain (encoded in amino acids 1-272). These transformants were screened on medium containing IPTG to induce two-hybrid protein expression and X-gal to detect interacting constructs. Prior to mutagenesis this strain would be blue on medium containing X-gal and IPTG (illustrated by high β-galactosidase activity in Figure 14). However, to screen for residues important for the FeoB-FeoC interaction, only white colonies were selected for further characterization.

If a mutation in *feoC* disrupted the structure of FeoC, it is possible that the protein would not be stable. Western blotting was performed to determine if T18-tagged FeoC was made using an antibody to the T18 fragment of adenylate cyclase. Only one strain made FeoC at levels similar to the non-mutagenized FeoC constructs (Figure 16). In β-

galactosidase assays this strain has low β-galactosidase activity (Figure 17), similar to the negative control, confirming the screening performed on solid medium for the loss of the interaction between FeoB and FeoC. Sequencing determined that the mutagenized *feoC* contains a single base pair mutation that changes the glutamate at position 29 to glycine.

To determine the conservation of glutamate 29, an alignment of amino acid sequences of FeoC proteins from *Vibrio* species, *E. coli,* and *Yersinia pestis* was performed (Figure 18A). In FeoC proteins from other *Vibrio* species glutamate 29 is conserved. Although the residue is not conserved *E. coli,* the *E. coli* and *V. cholerae* FeoC sequences are highly dissimilar, suggesting that *E. coli*-*V. cholerae* sequence comparisons cannot be used to draw conclusions about the importance of individual amino acids in the function of the protein (see Table 1). *Y. pestis* was included in the alignment because it is one of the few organisms on which mutation of *feoC* has been published. In *Y. pestis feoC* is dispensable for Feo function (87). Secondary structure predictions place glutamate 29 at the start of a helix in *V. cholerae* FeoC and the mutation to glycine does not alter the secondary structure in the immediate region of the amino acid substitution (Figure 18B). Effects of the substitution are seen downstream, where a region predicted to form a β-sheet in wild-type FeoC is instead predicted to form a helical region in FeoC-E29G. However, it is not know if these structural predictions are valid and whether they are important for either the FeoB-FeoC interaction or for Feo function.

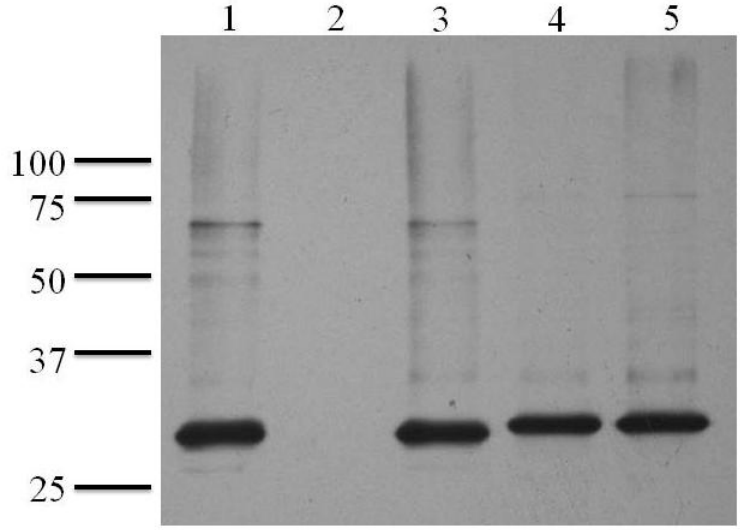

Figure 16. Detection of T18-tagged *V. cholerae* FeoC. *E. coli* BTH101 carrying plasmids described below was grown overnight at 30^{O}C with 0.5 mM IPTG to induce expression of the T18- and T25-tagged proteins. Equal numbers of cells were loaded on to a 10% SDS polyacryalmide gel. After electrophoresis, proteins were transferred to a nitrocellulose membrane and anti-CyaA antibody was used detected T18-tagged proteins. Lane 1: BTH101 pKT25-zip pUT18C-zip (positive control), Lane 2: BTH101 pKT25 pUT18C (negative control), Lane 3: BTH101 pKT25FeoB pUT18FeoC, Lane 4: BTH101 pKT25FeoB272 pUT18CFeoC, Lane 5: BTH101 pKT25FeoB272 pUT18CFeoC-E29G

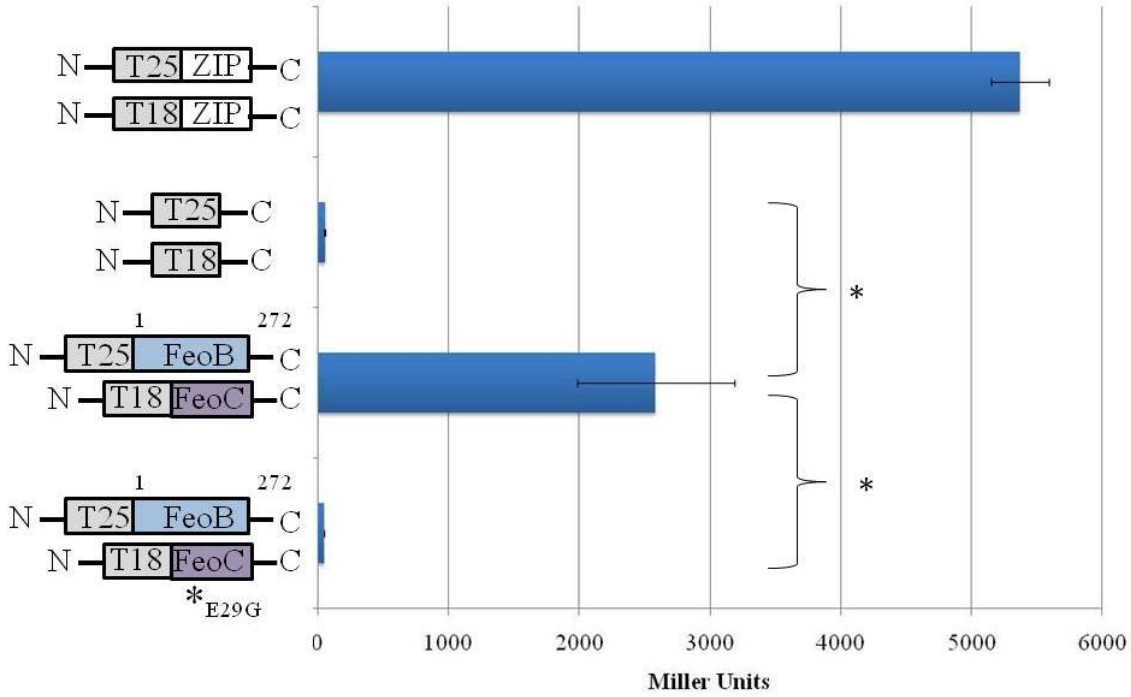

Figure 17. FeoC-E29G disrupts the interaction between *V. cholerae* FeoB and FeoC. *E. coli* BTH101 was grown overnight at 30^{O}C in 0.5 mM IPTG before performing a β-galactosidase assay (79). Strains tested are as follows, from top to bottom: BTH101 pKT25-zip pUT18C-zip (positive control), BTH101 pKT25 pUT18C (negative control), BTH101 pKT25FeoB272 pUT18CFeoC, BTH101 pKT25FeoB272 pUT18CFeoC-E29G. β-galactosidase activity is expressed as Miller Units. Shown is the average and standard deviation of three independent experiments. * P<0.002, determined by an unpaired Student's t-test.

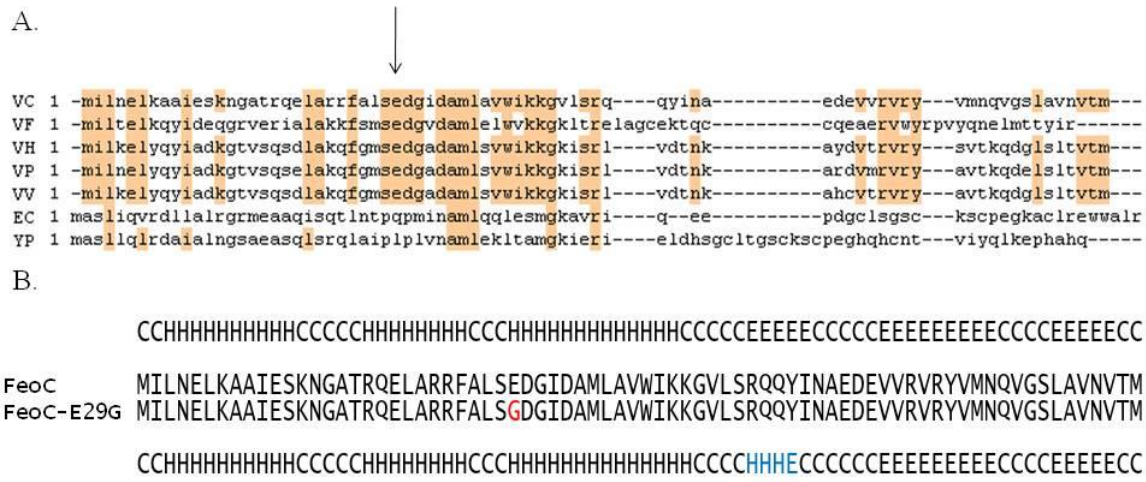

Figure 18. Amino acid sequence alignment of FeoC from different species and predicted secondary structure of FeoC and FeoC-E29G.

(A) Boxshade view of amino acid sequence alignment of FeoC from different species. VC, *V. cholerae*, VF, *Vibrio fischeri*, VH, *Vibrio harveyi*, VP, *Vibrio parahemolyticus*, VV, *Vibrio vulnificus*, EC, *E. coli*, YP, *Yersinia pestis*. Black arrow indicates position of glutamate 29 in *V. cholerae* FeoC. Shaded boxes represent >50% similarity. Alignment was performed using Clone Manager 9 software.

(B) The amino acid alignment of FeoC and FeoC-E29G with the glutamate change to glycine shown in red. Above and below the amino acid sequences are the secondary structure predictions for FeoC and FeoC-E29G, respectively. C=coil, H=helix, E=strand. The change in structure of FeoC-E29G is shown in blue. Alignment was performed with Porter (91).

6. Regulation of *V. cholerae feo* expression

In the human host, *V. cholerae* is found in the low oxygen environment of the human gastrointestinal tract. Low oxygen availability promotes ferrous iron availability and could act as a signal to *V. cholerae* that ferrous iron is present. Anaerobiosis has been shown to induce *feo* expression in *E. coli* (58). To determine if anaerobiosis stimulated *feo* expression in the enteric *V. cholerae, feoB* expression was measured by real time RT-PCR in aerobically and anaerobically grown *V. cholerae*. Consistent with results from *E. coli, V. cholerae feoB* expression is induced almost four-fold in anaerobic conditions (Figure 19).

Other conditions could regulate *V. cholerae feo* expression. To address this, Biolog phenotypic microarrays were used to screen a large number of conditions. Traditionally, phenotypic microarrays are used to determine the ability of a bacterium to use and metabolize substrates such as carbon, nitrogen, sulfur and phosphate sources and measure the organism's ability to grown in the presence of different osmolytes and pHs. As a consequence of metabolism, a tetrazolium dye is reduced and color production can be measured. In a modification of this assay, a *feo* promoter fusion to *lacZ* was constructed. Activation of *feo* expression could be monitored by replacing the tetrazolium dye with X-gal and measuring blue color production over time. Of the large number of conditions screened, only pH was found to regulate *feo* expression. As shown in Figure 20, the rate of blue color production, representative of *feo* expression, is faster at acid pH as compared to alkaline pH. After 24 hours of growth, *V. cholerae* reached a

similar A_{650}=1.4.-1.5 in pH 5.5 to pH 8.5. In pH 9.0 and higher, *V. cholerae* reached an A_{650}=1.2 after 24 hours of growth, indicating that in these pH range tested *V. cholerae* grew similarly.

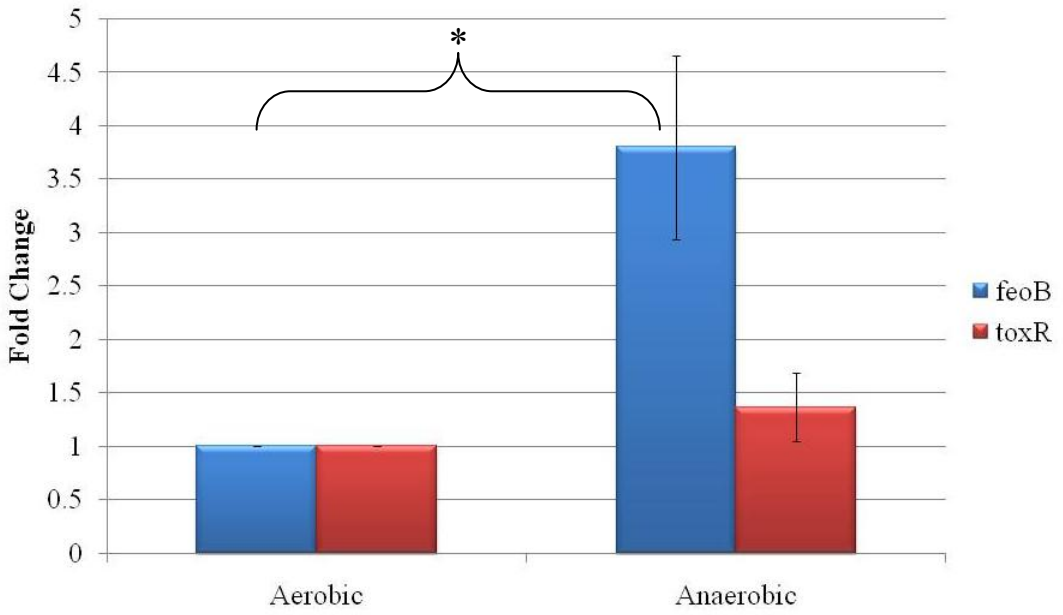

Figure 19. ***V. cholerae feoB*** **expression is anaerobically induced.** N16961-F was grown in EZ-RDM aerobically for 2.5 hours at 37^{O}C prior to splitting into two cultures. One culture was returned to aerobic growth condition while the second culture was placed into an anaerobic jar at 37^{O}C. Both cultures were grown for 1 hour prior to harvesting RNA. Real time RT-PCR was used to measure *feoB* expression and was normalized to *toxR* expression. Data shown is the means plus standard deviation for three independent experiments. * P<0.005, determined by an unpaired Student's t-test.

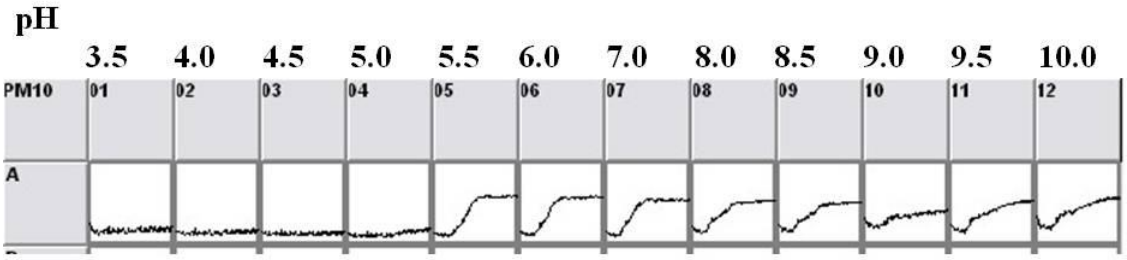

Figure 20. *V. cholerae feo* expression is induced in acidic pH. SAC500 carrying pQFeo, in which the *V. cholerae feo* promoter was fused to a promoterless *lacZ*, was monitored for 24 hours in a phenotypic microarray containing the chromogenic substrate X-gal. Color production, which is representative of *feo* expression, was measured and plotted over time. Shown is a portion of Biolog Plate PM10 plot of color production over time. Data were collected using OmniLog Data Collections Software.

IV. DISCUSSION

Vibrio cholerae is a pathogen that can be found in the human host and in the aquatic environment, locations in which *V. cholerae* is likely to experience iron limitation (104). In the human host, iron limitation is due to the sequestration of iron by host iron-binding proteins, a defense strategy that keeps this essential nutrient away from invading microbes (14). In the aquatic environment iron is scarce (3), making iron acquisition even more difficult. The more soluble, ferrous, form of iron is likely to predominate under conditions where oxygen is scarce and since brackish water, sediments, and the human intestinal tract are all likely to be low in oxygen ferrous iron may be the predominant form of iron available to *V. cholerae* in many of its ecological niches.

The *feoABC* operon encodes a major ferrous iron transporter and has been identified in many organisms, but the mechanism for iron transport via the Feo iron transport system remains poorly understood. Recently published studies focus on the G protein domain of FeoB, the probable ferrous permease, offering little data about the remainder of the protein. The contributions of FeoA and FeoC to iron transport have also largely been overlooked, leaving much of this iron transport system uncharacterized.

In this study, it was determined that FeoA, FeoB and FeoC are necessary for *V. cholerae* Feo-stimulated iron transport in iron transport mutants of *E. coli* and *S. flexneri*.

Although it has been suggested that FeoC may have a role in regulating expression of *feo* (20), neither FeoA nor FeoC were essential for *V. cholerae feoB* expression. These results shown here indicate that neither protein acts solely as a regulator of *feo* expression in *V. cholerae.* An approximate two-fold decrease in *feoB* expression was noted when an in-frame deletion was introduced in *feoA*; however, this decrease in *feoB* expression is not the source of the iron transport defect as the same amount of *feoB* expression was sufficient for iron transport when the deletion in *feoA* was complemented with *feoA in trans*. The reason for the decrease in *feoB* expression is not clear, and may be due to polar effects of the deletion in *feoA* on *feoB* or to a decrease in the stability of the message encoding *feoB* in the absence of a complete copy of *feoA* upstream.

To measure *feoB* expression, experiments were performed using a plasmid-based *V. cholerae feo* operon in a heterologous host. In this assay the *V. cholerae feo* operon is encoded on a low-copy-number vector, but expression of *feoB* from the plasmid may not be representative of levels of expression of chromosomal *feo* genes. In principle, a better method for testing if *feoA* or *feoC* is required for *feo* expression would be to measure *feoB* expression in *V. cholerae* containing chromosomal deletions in *feoA* or *feoC.* The problem with this experimental design, at this time, is that there is no phenotype for *V. cholerae feoB* mutants to determine if Feo is functional. This is most likely due to the multiple iron transport systems in *V. cholerae.* A final limitation with this experiment is that it is performed in a heterologous host. If either FeoA or FeoC required another *V.*

cholerae protein that is not conserved in *E. coli* H1771 for activity as a regulator, this requirement would be missed.

Previous characterization of FeoB has suggested it may act as a G protein. G proteins by themselves are often poor GTPases (10), requiring GAPs and GEFs to be efficient. Consistent with this requirement for effector proteins, FeoB has been characterized as having a slow rate of GTP hydrolysis and a fast, spontaneous rate of GDP release (73), suggesting that FeoB function is modulated by one or more effector proteins which stimulate GTP binding and hydrolysis. There are currently no known effector proteins that modulate the activity of the FeoB G protein domain in *V. cholerae* or any other organism. FeoA and FeoC are attractive candidates for this role, especially since they are not essential for *feoB* expression but are required for Feo-dependent ferrous iron transport. FeoA, which is predicted to contain an SH3-like domain (3) may act as a GEF for FeoB as SH3 domains are common in GEFs (10).

The hypothesis that FeoB requires effector proteins to regulate G protein activity is supported by BACTH results demonstrating that FeoC interacts with the cytoplasmic portion of FeoB. This is the first evidence that FeoB directly interacts with other proteins, although it is not known if this interaction is required for iron transport by Feo, it does provide evidence of a role for FeoC. *In vitro* biochemical tests will need to be performed to determine if FeoC stimulates GTP hydrolysis or affects nucleotide binding affinity, as sequence based predictions of GAP or GEF function can be difficult to make due to low conservation of structure and catalytic groups (10). It is possible the FeoC

does not act to modulate the proposed GTPase activity of FeoB, but plays another role entirely, possibly regulating FeoB via another mechanism or by acting more directly in iron transport.

Since the nature of the interaction between FeoC and FeoB may provide more insight into the role of each protein, random mutagenesis of FeoC was undertaken to identify residues or regions important for this interaction. A visual screen using BACTH was designed to allow identification of FeoC constructs that have lost the ability to interact with the cytoplasmic domain of FeoB (amino acids 1-272). A single base pair mutation in FeoC, resulting in the substitution of a glycine residue for a glutamate at position 29, disrupts the interaction between FeoB and FeoC (Figure 17). It is not clear if the glutamate residue itself is important in the interaction between FeoB and FeoC or if the substitution caused an alteration in the secondary structure of FeoC. Loss of the interaction between FeoC and FeoB was not a result of decreased stability of FeoC-E29G or reduced intracellular levels of the altered protein as the T18-tagged FeoC-E29G is made at comparable levels to other T18-tagged FeoC proteins.

Despite that fact that FeoC has been shown to be required for ferrous iron transport in *V. cholerae* and *E. coli* (20), not all organisms that contain a *feoB*-like gene have a downstream *feoC*, nor does FeoC appear to be required for ferrous iron transport by all organisms and under all conditions. In *Yersinia pestis* FeoC is dispensable for ferrous iron uptake under the conditions tested (87). Until basic characterization of additional *feo* operons is performed, and the genes required for Feo function are

identified, the basis for this discrepancy will not be understood. It is possible the function of FeoC is not required in some organisms that possess a functional Feo transporter. Additionally, it is possible that in some organisms the role of FeoC is filled by another protein. Finally, it is possible that *feoC* is actually present in most of the organisms that encode *feoB* but that many of the genomes have been misannotated, omitting *feoC* from the list of annotated genomes due both to its small size and recent description. Further characterization of other Feo-encoding organisms will assist in the understanding of the role of FeoC in ferrous iron transport.

The least characterized gene in the *feo* operon encodes FeoA, which is widespread among FeoB-encoding organisms (20), suggesting that it has an important role in ferrous iron acquisition. Very little is known about the structure and function of FeoA, with the exception of the predicted presence of an SH3-like domain within the protein (20). Proteins found to contain SH3-like domains are often implicated in protein-protein interactions and in the assembly of protein complexes, suggesting that FeoA forms interactions with other proteins, possibly FeoB or FeoC. Although no interactions between FeoA and FeoB or FeoC were observed using BACTH these do not rule out the possibility of interaction occurring in *V. cholerae in vivo,* as there are several limitations to the BACTH system used here. One major concern is whether proteins are folding properly in presence of the adenylate cyclase catalytic fragments.

During infection *V. cholerae* will be exposed to stimuli signaling the change in environments. Early in infection, *V. cholerae* must survive passage through the acidic

stomach to arrive at the low oxygen small intestine. The acidity in the stomach and the low oxygen concentration in the small intestine could act as signals both for ferrous iron availability and for the presence of the bacterium within the human host. In the gastrointestinal environment the *feo* genes have been shown to be some of the most highly expressed genes in vibrios shed from cholera patients (8) and vibrios recovered after infection of the rabbit ileal loop (119). Consistent with these previous findings, anaerobiosis and acidic pH, were each found to regulate *V. cholerae feo* expression allowing *V. cholerae* two methods of regulation expression of these important ferrous iron transporter through the lifecycle.

In this study, I used genetic methods to characterize the *V. cholerae feoABC* operon and its gene products. In *V. cholerae,* the Feo system was known to be involved in ferrous iron transport (117) but it was not known what genes were required for iron transport or what the roles of *feoA* or *feoC* were in iron transport. It is has yet to be shown that FeoB is in fact the ferrous permease for ferrous iron acquisition by Feo. *V. cholerae* Feo-mediated ferrous iron uptake in two heterologous iron mutants requires FeoA, FeoB and FeoC. FeoA and FeoC are not solely transcriptional regulators of the *feo* operon, finally addressing hypotheses put forth in the literature. More likely, these proteins participate in iron transport. Supporting this hypothesis in the demonstration that FeoC and the cytoplasmic domains of FeoB interact. Interactions between FeoC and FeoB have never been shown before. This result strongly suggests a direct role in iron transport for FeoC. Highly attractive candidate functions for FeoC include acting as a

GAP or GEF to regulate the G protein domain of FeoB. FeoC could have a different role in iron transport and may have additional functions. These findings have increased our understanding of the mode of ferrous iron transport in *V. cholerae*, a global pathogen. Further study into Feo will provide insight not only into ferrous iron transport but also evolutionary insight into bacterial G proteins and the primordial G protein cycle.

REFERENCES

1. 2010. WHO | Cholera. World Health Organization.

2. **Altschul S. F., W. Gish, W. Miller, E. W. Myers, and D. J. Lipman**. 1990. Basic local alignment search tool. Journal of Molecular Biology **215**:403-410.

3. **Andrews S. C., A. K. Robinson, and F. Rodríguez-Quiñones**. 2003. Bacterial iron homeostasis. FEMS Microbiology Reviews **27**:215-237.

4. **Aranda J., P. Cortes, M. E. Garrido, N. Fittipaldi, M. Llagostera, M. Gottschalk, and J. Barbe**. 2009. Contribution of the FeoB transporter to *Streptococcus suis* virulence. International Microbiology **12**:137-143.

5. **Ash M., A. Guilfoyle, R. J. Clarke, J. M. Guss, M. J. Maher, and M. Jormakka**. 2010. Potassium-activated GTPase Reaction in the G Protein-coupled Ferrous Iron Transporter B. Journal of Biological Chemistry **285**:14594 -14602.

6. **Atkin C. L., L. Thelander, P. Reichard, and G. Lang**. 1973. Iron and Free Radical in Ribonucleotide Reductase. Journal of Biological Chemistry **248**:7464 - 7472.

7. **Attridge S. R., E. Voss, and P. A. Manning**. 1993. The role of toxin-coregulated pili in the pathogenesis of *Vibrio cholerae* O1 El Tor. Microbial Pathogenesis **15**:421-431.

8. **Bina J., J. Zhu, M. Dziejman, S. Faruque, S. Calderwood, and J. Mekalanos**. 2003. ToxR regulon of *Vibrio cholerae* and its expression in vibrios shed by cholera patients. Proceedings of the National Academy of Sciences of the United States of America **100**:2801 -2806.

9. **Boguski M. S., and F. McCormick**. 1993. Proteins regulating Ras and its relatives. Nature **366**:643-654.

10. **Bos J. L., H. Rehmann, and A. Wittinghofer**. 2007. GEFs and GAPs: Critical Elements in the Control of Small G Proteins. Cell **129**:865-877.

11. **Bourne H. R., D. A. Sanders, and F. McCormick**. 1991. The GTPase superfamily: conserved structure and molecular mechanism. Nature **349**:117-127.

12. **Boyd J., M. N. Oza, and J. R. Murphy**. 1990. Molecular cloning and DNA sequence analysis of a diphtheria tox iron-dependent regulatory element (*dtxR*) from *Corynebacterium diphtheriae*. Proceedings of the National Academy of Sciences of

the United States of America **87**:5968 -5972.

13. **Brennan R., and B. Matthews**. 1989. The helix-turn-helix DNA binding motif. J Biol Chem **264**:1903-6.

14. **Bullen J. J., H. J. Rogers, P. B. Spalding, and C. G. Ward**. 2005. Iron and infection: the heart of the matter. FEMS Immunology and Medical Microbiology **43**:325-330.

15. **Burns R.** 1969. The nitrogenase system from *Azotobacter* Activation energy and divalent cation requirement. Biochimica et Biophysica Acta (BBA) - Enzymology **171**:253-259.

16. **Butterton J. R., J. A. Stoebner, S. M. Payne, and S. B. Calderwood**. 1992. Cloning, sequencing, and transcriptional regulation of *viuA*, the gene encoding the ferric vibriobactin receptor of *Vibrio cholerae*. J. Bacteriol. **174**:3729-3738.

17. **Cadwell R. C., and G. F. Joyce**. 1994. Mutagenic PCR. Genome Research **3**:S136 -S140.

18. **Calderwood S. B., and J. J. Mekalanos**. 1987. Iron regulation of Shiga-like toxin expression in *Escherichia coli* is mediated by the fur locus. J. Bacteriol. **169**:4759-4764.

19. **Cao J., M. R. Woodhall, J. Alvarez, M. L. Cartron, and S. C. Andrews**. 2007. EfeUOB (YcdNOB) is a tripartite, acid-induced and CpxAR-regulated, low-pH Fe2+ transporter that is cryptic in *Escherichia coli* K-12 but functional in *E. coli* O157:H7. Molecular Microbiology **65**:857-875.

20. **Cartron M., S. Maddocks, P. Gillingham, C. Craven, and S. Andrews**. 2006. Feo – Transport of Ferrous Iron into Bacteria. BioMetals **19**:143-157.

21. **Cassel D., and T. Pfeuffer**. 1978. Mechanism of cholera toxin action: Covalent modification of the guanyl nucleotide-binding protein of the adenylate cyclase system. Proceedings of the National Academy of Sciences of the United States of America **75**:2669 -2673.

22. **Chang A. C., and S. N. Cohen**. 1978. Construction and characterization of amplifiable multicopy DNA cloning vehicles derived from the P15A cryptic miniplasmid. J. Bacteriol. **134**:1141-1156.

23. **Chappell P. D., and E. A. Webb**. 2010. A molecular assessment of the iron stress response in the two phylogenetic clades of *Trichodesmium*. Environmental

Microbiology **12**:13-27.

24. **Choi E., E. A. Groisman, and D. Shin**. 2009. Activated by Different Signals, the PhoP/PhoQ Two-Component System Differentially Regulates Metal Uptake. J. Bacteriol. **191**:7174-7181.

25. **Colwell R. R., J. Kaper, and S. W. Joseph**. 1977. *Vibrio cholerae*, *Vibrio parahaemolyticus*, and Other *Vibrios*: Occurrence and Distribution in Chesapeake Bay. Science **198**:394-396.

26. **Coy M., and J. B. Neilands**. 1991. Structural dynamics and functional domains of the Fur protein. Biochemistry **30**:8201-8210.

27. **Cuatrecasas P.** 1973. Gangliosides and membrane receptors for cholera toxin. Biochemistry **12**:3558-3566.

28. **D'Aquino J. A., and D. Ringe**. 2003. Determinants of the Src Homology Domain 3-Like Fold. J. Bacteriol. **185**:4081-4086.

29. **Dashper S. G., C. A. Butler, J. P. Lissel, R. A. Paolini, B. Hoffmann, P. D. Veith, N. M. O'Brien-Simpson, S. L. Snelgrove, J. T. Tsiros, and E. C. Reynolds**. 2005. A Novel *Porphyromonas gingivalis* FeoB Plays a Role in Manganese Accumulation. Journal of Biological Chemistry **280**:28095 -28102.

30. **De Vos A. M., L. Tong, M. V. Milburn, P. M. Matias, J. Jancarik, S. Noguchi, S. Nishimura, K. Miura, E. Ohtsuka, and S. Kim**. 1988. Three-dimensional structure of an oncogene protein: catalytic domain of human c-H-ras p21. Science.

31. **Eng E. T., A. R. Jalilian, K. A. Spasov, and V. M. Unger**. 2008. Characterization of a Novel Prokaryotic GDP Dissociation Inhibitor Domain from the G Protein Coupled Membrane Protein FeoB. Journal of Molecular Biology **375**:1086-1097.

32. **Farinha M. A., and A. M. Kropinski**. 1990. Construction of broad-host-range plasmid vectors for easy visible selection and analysis of promoters. J. Bacteriol. **172**:3496-3499.

33. **Faruque S. M., M. J. Albert, and J. J. Mekalanos**. 1998. Epidemiology, Genetics, and Ecology of Toxigenic *Vibrio cholerae*. Microbiol. Mol. Biol. Rev. **62**:1301-1314.

34. **Fisher C. R., N. M. L. L. Davies, E. E. Wyckoff, Z. Feng, E. V. Oaks, and S. M. Payne**. 2009. Genetics and Virulence Association of the *Shigella flexneri* Sit Iron Transport System. Infect. Immun. **77**:1992-1999.

35. **Fleming T. P., M. S. Nahlik, and M. A. McIntosh**. 1983. Regulation of enterobactin iron transport in *Escherichia coli*: characterization of *ent*::Mu d(Apr *lac*) operon fusions. J. Bacteriol. **156**:1171-1177.

36. **Forth W., and W. Rummel**. 1973. Iron absorption. Physiol. Rev. **53**:724-792.

37. **Geider R., and J. Roche**. 1994. The role of iron in phytoplankton photosynthesis, and the potential for iron-limitation of primary productivity in the sea. Photosynthesis Research **39**:275-301.

38. **Gill D. M., and R. Meren**. 1978. ADP-ribosylation of membrane proteins catalyzed by cholera toxin: basis of the activation of adenylate cyclase. Proceedings of the National Academy of Sciences of the United States of America **75**:3050 -3054.

39. **Grass G., S. Franke, N. Taudte, D. H. Nies, L. M. Kucharski, M. E. Maguire, and C. Rensing**. 2005. The Metal Permease ZupT from *Escherichia coli* Is a Transporter with a Broad Substrate Spectrum. J. Bacteriol. **187**:1604-1611.

40. **Grass G., M. D. Wong, B. P. Rosen, R. L. Smith, and C. Rensing**. 2002. ZupT Is a Zn(II) Uptake System in *Escherichia coli*. J. Bacteriol. **184**:864-866.

41. **Griffiths G. L., S. P. Sigel, S. M. Payne, and J. B. Neilands**. 1984. Vibriobactin, a siderophore from *Vibrio cholerae*. Journal of Biological Chemistry **259**:383 -385.

42. **Große C., J. Scherer, D. Koch, M. Otto, N. Taudte, and G. Grass**. 2006. A new ferrous iron-uptake transporter, EfeU (YcdN), from *Escherichia coli*. Molecular Microbiology **62**:120-131.

43. **Guilfoyle A., M. J. Maher, M. Rapp, R. Clarke, S. Harrop, and M. Jormakka**. 2009. Structural basis of GDP release and gating in G protein coupled Fe2+ transport. EMBO J **28**:2677-2685.

44. **Halliwell B., and J. M. C. Gutteridge**. 1992. Biologically relevant metal ion-dependent hydroxyl radical generation An update. FEBS Letters **307**:108-112.

45. **Hantke K.** 1984. Cloning of the repressor protein gene of iron-regulated systems in *Escherichia coli* K12. Molecular and General Genetics MGG **197**:337-341.

46. **Hantke K.** 1987. Ferrous iron transport mutants in *Escherichia coli* K12. FEMS Microbiology Letters **44**:53-57.

47. **Hantke K.** 1981. Regulation of ferric iron transport in *Escherichia coli* K12: Isolation of a constitutive mutant. Molecular and General Genetics MGG **182**:288-292.

48. **Hattori M., Y. Jin, H. Nishimasu, Y. Tanaka, M. Mochizuki, T. Uchiumi, R. Ishitani, K. Ito, and O. Nureki**. 2009. Structural Basis of Novel Interactions Between the Small-GTPase and GDI-like Domains in Prokaryotic FeoB Iron Transporter. Structure **17**:1345-1355.

49. **Henderson D. P., and S. M. Payne**. 1994. Characterization of the *Vibrio cholerae* outer membrane heme transport protein HutA: sequence of the gene, regulation of expression, and homology to the family of TonB-dependent proteins. J. Bacteriol. **176**:3269-3277.

50. **Henderson D. P., and S. M. Payne**. 1993. Cloning and characterization of the *Vibrio cholerae* genes encoding the utilization of iron from haemin and haemoglobin. Molecular Microbiology **7**:461-469.

51. **Herrington D. A., R. H. Hall, G. Losonsky, J. J. Mekalanos, R. K. Taylor, and M. M. Levine**. 1988. Toxin, toxin-coregulated pili, and the *toxR* regulon are essential for *Vibrio cholerae* pathogenesis in humans. The Journal of Experimental Medicine **168**:1487 -1492.

52. **Higgs P. I., P. S. Myers, and K. Postle**. 1998. Interactions in the TonB-Dependent Energy Transduction Complex: ExbB and ExbD Form Homomultimers. J. Bacteriol. **180**:6031-6038.

53. **Hirose S., N. Yaginuma, and Y. Inada**. 1974. Disruption of charge separation followed by that of the proteon gradient in the mitochondrial membrane by CCCP. J. Biochem **76**:213-216.

54. **Hung K., Y. Chang, E. T. Eng, J. Chen, Y. Chen, Y. Sun, C. Hsiao, G. Dong, K. A. Spasov, V. M. Unger, and T. Huang**. 2010. Structural fold, conservation and Fe(II) binding of the intracellular domain of prokaryote FeoB. Journal of Structural Biology **170**:501-512.

55. **Huq A., E. B. Small, P. A. West, M. I. Huq, R. Rahman, and R. R. Colwell**. 1983. Ecological Relationships between *Vibrio cholerae* and Planktonic Crustacean Copepods. Applied and Environmental Microbiology **45**:275-283.

56. **Jeon J., H. Kim, J. Yun, S. Ryu, E. A. Groisman, and D. Shin**. 2008. RstA-Promoted Expression of the Ferrous Iron Transporter FeoB under Iron-Replete Conditions Enhances Fur Activity in Salmonella enterica. J. Bacteriol. **190**:7326-7334.

57. **Jin B., S. M. C. Newton, Y. Shao, X. Jiang, A. Charbit, and P. E. Klebba**. 2006. Iron acquisition systems for ferric hydroxamates, haemin and haemoglobin in *Listeria monocytogenes*. Molecular Microbiology **59**:1185-1198.

58. **Kammler M., C. Schon, and K. Hantke**. 1993. Characterization of the ferrous iron uptake system of *Escherichia coli*. J. Bacteriol. **175**:6212-6219.

59. **Kaper J., J. Morris, and M. Levine**. 1995. Cholera. Clin. Microbiol. Rev. **8**:48-86.

60. **Karimova G., N. Dautin, and D. Ladant**. 2005. Interaction Network among *Escherichia coli* Membrane Proteins Involved in Cell Division as Revealed by Bacterial Two-Hybrid Analysis. J. Bacteriol. **187**:2233-2243.

61. **Karimova G., J. Pidoux, A. Ullmann, and D. Ladant**. 1998. A bacterial two-hybrid system based on a reconstituted signal transduction pathway. Proceedings of the National Academy of Sciences of the United States of America **95**:5752 -5756.

62. **Katoh H., N. Hagino, A. R. Grossman, and T. Ogawa**. 2001. Genes Essential to Iron Transport in the Cyanobacterium *Synechocystis* sp. Strain PCC 6803. J. Bacteriol. **183**:2779-2784.

63. **Kehres D. G., M. L. Zaharik, B. B. Finlay, and M. E. Maguire**. 2000. The NRAMP proteins of *Salmonella typhimurium* and *Escherichia coli* are selective manganese transporters involved in the response to reactive oxygen. Molecular Microbiology **36**:1085-1100.

64. **Kehres D. G., A. Janakiraman, J. M. Slauch, and M. E. Maguire**. 2002. SitABCD Is the Alkaline Mn2+ Transporter of *Salmonella enterica* Serovar Typhimurium. J. Bacteriol. **184**:3159-3166.

65. **Koster S., W. Kuhlbrandt, and O. Yildiz**. 2009. Purification, crystallization and preliminary X-ray diffraction analysis of the FeoB G domain from *Methanococcus jannaschii*. Acta Crystallographica Section F **65**:684-687.

66. **Koster S., M. Wehner, C. Herrmann, W. Kuhlbrandt, and O. Yildiz**. 2009. Structure and Function of the FeoB G-Domain from *Methanococcus jannaschii*. Journal of Molecular Biology **392**:405-419.

67. **Lambden P. R., and J. R. Guest**. 1976. Mutants of *Escherichia coli* K12 Unable to use Fumarate as an Anaerobic Electron Acceptor. J Gen Microbiol **97**:145-160.

68. **Lazazzera B. A., H. Beinert, N. Khoroshilova, M. C. Kennedy, and P. J. Kiley**. 1996. DNA Binding and Dimerization of the Fe−S-containing FNR Protein from *Escherichia coli* Are Regulated by Oxygen. Journal of Biological Chemistry **271**:2762 -2768.

69. **Louvel H., I. Saint Girons, and M. Picardeau**. 2005. Isolation and Characterization of FecA- and FeoB-Mediated Iron Acquisition Systems of the Spirochete *Leptospira biflexa* by Random Insertional Mutagenesis. J. Bacteriol. **187**:3249-3254.

70. **Mademidis A., H. Killmann, W. Kraas, I. Flechsler, G. Jung, and V. Braun**. 1997. ATP-dependent ferric hydroxamate transport system in *Escherichia coli*: periplasmic FhuD interacts with a periplasmic and with a transmembrane/cytoplasmic region of the integral membrane protein FhuB, as revealed by competitive peptide mapping. Molecular Microbiology **26**:1109-1123.

71. **Makui H., E. Roig, S. T. Cole, J. D. Helmann, P. Gros, and M. F. M. Cellier**. 2000. Identification of the *Escherichia coli* K-12 Nramp orthologue (MntH) as a selective divalent metal ion transporter. Molecular Microbiology **35**:1065-1078.

72. **Marinus M. G., and E. B. Konrad**. 1976. Hyper-recombination in *dam* mutants of *Escherichia coli* K-12. Molecular and General Genetics MGG **149**:273-277-277.

73. **Marlovits T. C., W. Haase, C. Herrmann, S. G. Aller, and V. M. Unger**. 2002. The membrane protein FeoB contains an intramolecular G protein essential for Fe(II) uptake in bacteria. Proceedings of the National Academy of Sciences of the United States of America **99**:16243 -16248.

74. **Meibom K. L., X. B. Li, A. T. Nielsen, C. Wu, S. Roseman, and G. K. Schoolnik**. 2004. The *Vibrio cholerae* chitin utilization program. Proceedings of the National Academy of Sciences of the United States of America **101**:2524 -2529.

75. **Merrell D. S., S. M. Butler, F. Qadri, N. A. Dolganov, A. Alam, M. B. Cohen, S. B. Calderwood, G. K. Schoolnik, and A. Camilli**. 2002. Host-induced epidemic spread of the cholera bacterium. Nature **417**:642-645.

76. **Mey A. R., and S. M. Payne**. 2001. Haem utilization in *Vibrio cholerae* involves multiple TonB-dependent haem receptors. Molecular Microbiology **42**:835-849.

77. **Mey A. R., E. E. Wyckoff, L. A. Hoover, C. R. Fisher, and S. M. Payne**. 2008.

Vibrio cholerae VciB Promotes Iron Uptake via Ferrous Iron Transporters. J. Bacteriol. **190**:5953-5962.

78. **Mey A. R., E. E. Wyckoff, A. G. Oglesby, E. Rab, R. K. Taylor, and S. M. Payne**. 2002. Identification of the *Vibrio cholerae* Enterobactin Receptors VctA and IrgA: IrgA Is Not Required for Virulence. Infect. Immun. **70**:3419-3426.

79. **Miller J. H.** 1972. Experiments in molecular genetics. Cold Spring Harbor Laboratory Press, Cold Spring Harbor, N.Y.

80. **Neidhardt F. C., P. L. Bloch, and D. F. Smith**. 1974. Culture Medium for Enterobacteria. J. Bacteriol. **119**:736-747.

81. **Neilands J. B.** 1981. Iron Absorption and Transport in Microorganisms. Annual Review of Nutrition **1**:27-46.

82. **Neilands J. B.** 1981. Microbial Iron Compounds. Annual Review of Biochemistry **50**:715-731.

83. **Occhino D. A., E. E. Wyckoff, D. P. Henderson, T. J. Wrona, and S. M. Payne**. 1998. *Vibrio cholerae* iron transport: haem transport genes are linked to one of two sets of *tonB, exbB, exbD* genes. Molecular Microbiology **29**:1493-1507.

84. **Pandey A., and R. V. Sonti**. 2010. Role of the FeoB Protein and Siderophore in Promoting Virulence of *Xanthomonas oryzae* pv. oryzae on Rice. J. Bacteriol. **192**:3187-3203.

85. **Payne S. M., and R. A. Finkelstein**. 1978. Siderophore production by *Vibrio cholerae*. Infect. Immun. **20**:310-311.

86. **Payne S. M., and A. R. Mey**. 2004. Pathogenic *Escherichia coli*, *Shigella*, and *Salmonella*, pp. 199-218. *In* Iron transport in bacteria. ASM Press, Washington, DC.

87. **Perry R., I. Mier, and J. Fetherston**. 2007. Roles of the Yfe and Feo transporters of *Yersinia pestis* in iron uptake and intracellular growth. BioMetals **20**:699-703.

88. **Petermann N., G. Hansen, C. L. Schmidt, and R. Hilgenfeld**. 2010. Structure of the GTPase and GDI domains of FeoB, the ferrous iron transporter of *Legionella pneumophila*. FEBS Letters **584**:733-738.

89. **Peterson J. D., L. A. Umayam, T. Dickinson, E. K. Hickey, and O. White**. 2001. The Comprehensive Microbial Resource. Nucleic Acids Research **29**:123 -125.

90. **Pohl E., J. C. Haller, A. Mijovilovich, W. Meyer-Klaucke, E. Garman, and M. L. Vasil**. 2003. Architecture of a protein central to iron homeostasis: crystal structure and spectroscopic analysis of the ferric uptake regulator. Molecular Microbiology **47**:903-915.

91. **Pollastri G., and A. McLysaght**. Porter: a new, accurate server for protein secondary structure prediction. Bioinformatics **21**:1719 -1720.

92. **Postle K.** 1993. TonB protein and energy transduction between membranes. Journal of Bioenergetics and Biomembranes **25**:591-601.

93. **Puig O., F. Caspary, G. Rigaut, B. Rutz, E. Bouveret, E. Bragado-Nilsson, M. Wilm, and B. Seraphin**. 2001. The Tandem Affinity Purification (TAP) Method: A General Procedure of Protein Complex Purification. Methods **24**:218-229.

94. **Reynolds P. R., G. P. Mottur, and C. Bradbeer**. 1980. Transport of vitamin B12 in *Escherichia coli*. Some observations on the roles of the gene products of BtuC and TonB. Journal of Biological Chemistry **255**:4313 -4319.

95. **Rigaut G., A. Shevchenko, B. Rutz, M. Wilm, M. Mann, and B. Seraphin**. 1999. A generic protein purification method for protein complex characterization and proteome exploration. Nat Biotech **17**:1030-1032.

96. **Robey M., and N. P. Cianciotto**. 2002. *Legionella pneumophila* feoAB Promotes Ferrous Iron Uptake and Intracellular Infection. Infect. Immun. **70**:5659-5669.

97. **Rogers H. J.** 1973. Iron-Binding Catechols and Virulence in *Escherichia coli*. Infect. Immun. **7**:445-456.

98. **Rohrbach M., V. Braun, and W. Koster**. 1995. Ferrichrome transport in *Escherichia coli* K-12: altered substrate specificity of mutated periplasmic FhuD and interaction of FhuD with the integral membrane protein FhuB. J. Bacteriol. **177**:7186-7193.

99. **Runyen-Janecky L. J., S. A. Reeves, E. G. Gonzales, and S. M. Payne**. 2003. Contribution of the *Shigella flexneri* Sit, Iuc, and Feo Iron Acquisition Systems to Iron Acquisition In Vitro and in Cultured Cells. Infect. Immun. **71**:1919-1928.

100. **Saha P., H. Koley, A. Mukhopadhyay, S. Bhattacharya, G. Nair, B. Ramakrishnan, S. Krishnan, T. Takeda, and Y. Takeda**. 1996. Nontoxigenic *Vibrio cholerae* 01 serotype Inaba biotype El Tor associated with a cluster of cases of cholera in southern India. J. Clin. Microbiol. **34**:1114-1117.

101. **Sambrook J., and D. W. Russell**. 2001. Molecular cloning: a laboratory manual. Cold Spring Harbor Laboratory Press, Cold Spring Harbor, N.Y.

102. **Seliger S. S., A. R. Mey, A. Valle, and S. M. Payne**. 2001. The two TonB systems of *Vibrio cholerae*: redundant and specific functions. Molecular Microbiology **39**:801-812.

103. **Sharma C., M. Thungapathra, A. Ghosh, A. K. Mukhopadhyay, A. Basu, R. Mitra, I. Basu, S. K. Bhattacharya, T. Shimada, T. Ramamurthy, T. Takeda, S. Yamasaki, Y. Takeda, and G. B. Nair**. 1998. Molecular Analysis of Non-O1, Non-O139 *Vibrio cholerae* Associated with an Unusual Upsurge in the Incidence of Cholera-Like Disease in Calcutta, India. J. Clin. Microbiol. **36**:756-763.

104. **Sigel S. P., and S. M. Payne**. 1982. Effect of iron limitation on growth, siderophore production, and expression of outer membrane proteins of *Vibrio cholerae*. J. Bacteriol. **150**:148-155.

105. **Simon E. H., and I. Tessman**. Thymidine-requiring mutants of phage T4. Proceedings of the National Academy of Sciences of the United States of America **50**:526-532.

106. **Spira W. M., A. Huq, Q. S. Ahmed, and Y. A. Saeed**. 1981. Uptake of *Vibrio cholerae* Biotype eltor from Contaminated Water by Water Hyacinth (Eichornia crassipes). Applied and Environmental Microbiology **42**:550-553.

107. **Sprang S. R.** 1997. G proteins, effectors and GAPs: structure and mechanism. Current Opinion in Structural Biology **7**:849-856.

108. **Tamplin M. L., A. L. Gauzens, A. Huq, D. A. Sack, and R. R. Colwell**. 1990. Attachment of *Vibrio cholerae* serogroup O1 to zooplankton and phytoplankton of Bangladesh waters. Applied and Environmental Microbiology **56**:1977-1980.

109. **Taudte N., and G. Grass**. 2010. Point mutations change specificity and kinetics of metal uptake by ZupT from *Escherichia coli*. BioMetals **23**:643-656.

110. **Taylor R. K., V. L. Miller, D. B. Furlong, and J. J. Mekalanos**. 1987. Use of *phoA* gene fusions to identify a pilus colonization factor coordinately regulated with cholera toxin. Proceedings of the National Academy of Sciences of the United States of America **84**:2833 -2837.

111. **Touati D.** 2000. Iron and Oxidative Stress in Bacteria. Archives of Biochemistry and Biophysics **373**:1-6.

112. **Tsolis R., A. Baumler, F. Heffron, and I. Stojiljkovic**. 1996. Contribution of TonB- and Feo-mediated iron uptake to growth of *Salmonella typhimurium* in the mouse. Infect. Immun. **64**:4549-4556.

113. **Velayudhan J., N. J. Hughes, A. A. McColm, J. Bagshaw, C. L. Clayton, S. C. Andrews, and D. J. Kelly**. 2000. Iron acquisition and virulence in *Helicobacter pylori*: a major role for FeoB, a high-affinity ferrous iron transporter. Molecular Microbiology **37**:274-286.

114. **Wang R. F., and S. R. Kushner**. 1991. Construction of versatile low-copy-number vectors for cloning, sequencing and gene expression in *Escherichia coli*. Gene **100**:195-199.

115. **Watnick P. I., and R. Kolter**. 1999. Steps in the development of a *Vibrio cholerae* El Tor biofilm. Molecular Microbiology **34**:586-595.

116. **Wyckoff E., A. Mey, and S. Payne**. 2007. Iron acquisition in *Vibrio cholerae*. BioMetals **20**:405-416.

117. **Wyckoff E. E., A. R. Mey, A. Leimbach, C. F. Fisher, and S. M. Payne**. 2006. Characterization of Ferric and Ferrous Iron Transport Systems in *Vibrio cholerae*. J. Bacteriol. **188**:6515-6523.

118. **Wyckoff E. E., A. Valle, S. L. Smith, and S. M. Payne**. 1999. A Multifunctional ATP-Binding Cassette Transporter System from *Vibrio cholerae* Transports Vibriobactin and Enterobactin. J. Bacteriol. **181**:7588-7596.

119. **Xu Q., M. Dziejman, and J. J. Mekalanos**. 2003. Determination of the transcriptome of *Vibrio cholerae* during intraintestinal growth and midexponential phase in vitro. Proceedings of the National Academy of Sciences of the United States of America **100**:1286 -1291.

120. **Zhou D., W. Hardt, and J. E. Galan**. 1999. Salmonella typhimurium Encodes a Putative Iron Transport System within the Centisome 63 Pathogenicity Island. Infect. Immun. **67**:1974-1981.

121. **Zhu J., and J. J. Mekalanos**. 2003. Quorum Sensing-Dependent Biofilms Enhance Colonization in *Vibrio cholerae*. Developmental Cell **5**:647-656.

122. **Zuker M.** 2003. Mfold web server for nucleic acid folding and hybridization prediction. Nucleic Acids Research **31**:3406 -3415.

VITA

Emily Ann Helton was born in Englewood, Colorado March 28th, 1982. She attended Hastings College in Hastings, Nebraska from August 2000 until May 2003. She then transferred to the University of Nebraska Medical Center in Omaha, Nebraska and graduated with a B.S. in Medical Technology in May 2004. In August of 2004, she began her studies at the University of Texas at Austin.

Permanent email Address: emilyhelton@yahoo.com

This dissertation was typed by the author.